UNIVERSITY OF OKLAHOMA

GRADUATE COLLEGE

IMPACT OF VISCOUS ACID-IN-OIL EMULSION FORMATION ON WELL PRODUCTIVITY FOLLOWING ACID STIMULATION

A THESIS

SUBMITTED TO THE GRADUATE FACULTY

in partial fulfillment of the requirements for the

Degree of

MASTER OF SCIENCE

By

BRYAN SCARBOROUGH
Norman, Oklahoma
2016

IMPACT OF VISCOUS ACID-IN-OIL EMULSION FORMATION ON WELL PRODUCTIVITY FOLLOWING ACID STIMULATION

A THESIS APPROVED FOR THE
MEWBOURNE SCHOOL OF PETROLEUM AND GEOLOGICAL ENGINEERING

BY

_____
Dr. Mashhad Fahes, Chair

_____
Dr. Maysam Pournik

_____
Dr. Ahmad Sakhaee-Pour

© Copyright by BRYAN SCARBOROUGH 2016
All Rights Reserved.

Acknowledgements

I would like to thank my committee chair, Dr. Fahes, for her unwavering encouragement and enthusiastic support throughout the course of this research. I would also like to express my gratitude to Dr. Pournik for his support and valued input as this study would not have been completed otherwise. Thank you to Dr. Sakhaee-Pour for serving on my thesis committee and for your valuable feedback.

I would also like to thank Dr. Firoozabadi for hosting me as a summer 2015 intern at the Reservoir Engineering Institute; I learned a lot and our work during the internship has served as a starting point for the current research. In addition, I would like to thank Valentina and Mohamed for their help in the lab.

Thanks to my friends and colleagues at University of Oklahoma who have supported me along the way.

Table of Contents

List of Tables

List of Figures

Abstract

Acid stimulation techniques matrix acidizing and acid fracturing are commonly applied in carbonate reservoirs. The goal of such techniques is to increase well productivity by enhancing permeability in the near wellbore area. Frequently, these stimulation techniques can introduce formation damage such as sludge formation or viscous emulsions resulting in lower than expected well productivity enhancement or well productivity reduction, sometimes irreversible. This study will focus on the formation of viscous acid-in-crude emulsion formation and its effect on well productivity.

Emulsion bottle testing experiments with 15% hydrochloric acid (HCl) and a North Texas Crude oil have been performed to study the effect of acid fraction and time on emulsion viscosity and stability. Also, acid coreflooding experiments have been conducted to study the in-situ formation of acid-in-crude emulsions and the effect on subsequent oil injection.

Bottle testing results indicate that emulsion viscosity increases dramatically with increasing acid fraction; viscosities of over 1000 cP have been measured. Emulsion viscosity also increases with time as a separation of free oil and emulsion occurs; the separated emulsion has a higher acid fraction than the initial mix and is extremely viscous, nearly solid-like.

Acid coreflooding results show direct evidence of acid-in-crude emulsion formation on crude-saturated cores. Viscosity of one such emulsion was measured at 860 cP and was shown to be extremely stable. Coreflooding tests with an acid injection

period followed by an oil injection period could not indicate if in-situ emulsion formation during acid injection has a detrimental effect on subsequent oil production.

CHAPTER 1: INTRODUCTION AND LITERATURE REVIEW

Acid Stimulation

Acid stimulation of oil and gas reservoirs, with the goal of increasing well productivity has been applied since the late 19th century. Matrix acid stimulation and acid fracturing are the two types of acid stimulation. Acid stimulation is usually reserved for carbonate reservoirs although matrix acid stimulation of sandstone reservoirs does occur less frequently.

Near-wellbore permeability is usually impaired in conventional overbalanced drilling operations and completion operations. Small solid particles in the drilling fluid invade the formation and reduce the permeability in the near-wellbore area. Fluid invasion may also lead to a reduction of effective permeability to hydrocarbons via relative permeability effects. The result of these processes is called formation damage and the area around the well impacted is called the damaged zone. Formation damage leads to a greater than ideal pressure drop near the well and can significantly decrease the well productivity. The deviation from an ideal pressure drop near the well is quantified in the skin factor. A skin factor greater than 0 indicates some type of formation damage and a skin factor less than zero indicates increased near-wellbore permeability. The goal of acid stimulation is to bypass the damaged zone or increase the near-wellbore permeability of a non-damaged well. When successful, the stimulation job will result in a decrease skin and increased well productivity.

Carbonate matrix acidizing is a stimulation technique in which acid, usually hydrochloric acid (HCl), is injected into the formation below the fracture pressure to dissolve the calcium carbonate ($CaCO_3$) matrix rock. The chemical reaction is:

$$2HCl + CaCO_3 \rightarrow CaCl_2 + H_20 + CO_2$$

The goal is to create high permeability channels, known as wormholes, with an emphasis on maximizing the length of created wormholes. Ideally, the wormholes will penetrate beyond the damaged zone, and in this case the skin factor can be calculated as:

$$s = -ln\left(\frac{r_{wh}}{r_w}\right)$$

$$where \quad s = skin, \ r_{wh} = wormhole\ length, \ r_w = wellbore\ radius$$

Acid fracturing is the process of injecting acid into a carbonate formation above the rock fracture pressure, creating a hydraulic fracture in the rock. The acid creates a differential etched pattern on the fracture faces which results in a higher conductivity flow path along the fracture upon closure. Success depends on the etched fracture length and the retained conductivity under load. Conductivity of the fracture is a function of the amount of face dissolution, the pattern of dissolution, the strength of the fracture faces, and the closure stress. A high conductivity fracture requires non-uniform surface etching and sufficient fracture strength.

While the goal of acid stimulation is to overcome formation damage, a risk is introducing additional formation damage, sometimes irreversibly. Formation damage associated with acid stimulation, resulting from sludge formation or viscous emulsions for example, is well documented. This investigation focuses on formation damage caused by viscous emulsions during acidizing operations, although the problems of viscous emulsion formation and sludge formation are related.

Emulsions

An emulsion is a dispersion of one liquid in another immiscible liquid. The phase that is dispersed in the form of droplets is called the dispersed or internal phase, and the phase in which the droplets are suspended is called the continuous or external phase. In oilfield emulsions, one of the phases is aqueous and the other is crude oil. Emulsions occur in almost all phases of oil production and processing: in reservoirs, wellbores, wellheads, surface facilities, transportation pipelines, crude storage facilities, and petroleum processing facilities.

From a thermodynamic perspective, oilfield emulsions are unstable systems. There is a natural tendency for a liquid/liquid system to separate and reduce its interfacial area and, thus, its interfacial energy. But most emulsions are stable over a period of time, or in other words they possess kinetic stability. Produced oilfield emulsions are categorized based on their degree of kinetic stability (Kokal 2005):

- Loose emulsions – separate in a matter of minutes
- Medium emulsions – separate in 10 minutes or more
- Tight emulsions – will separate (sometimes only partially) in a matter of hours or even days

Oilfield emulsions can also be classified into three main groups: water-in-oil (W/O), oil-in-water (O/W), and multiple or complex emulsions. W/O emulsions consist of water droplets dispersed in a continuous oil phase and O/W emulsions consist of oil droplets in a continuous water phase. In multiple or complex emulsions, tiny droplets are dispersed in larger droplets which are dispersed in a continuous phase. For example, a W/O/W emulsion consists of water droplets dispersed in larger oil droplets

which are dispersed in a continuous water phase. Produced oilfield emulsions tend to be W/O emulsions up to very high water cuts. At approximately 80% water cut, the W/O emulsion inverts to an O/W emulsion and the dispersed water phase becomes the continuous phase (Kokal 2005).

For the purposes of this investigation we will focus on W/O emulsions that form in the reservoir during acid stimulation processes. These emulsions are often very viscous and have the potential to negatively impact well productivity. There are many reports in the literature of such cases.

Field Examples of Emulsions from Acidizing

Dunlap and Houchin performed a field study in which acid returns were examined via polarized microscopy for 32 wells in Alaska, California, and the Gulf of Mexico (Dunlap and Houchin 1990). Although precautions were used to prevent emulsions in each of the 32 studied wells, emulsions to some degree were evident in each case. The acid induced emulsions ranged from severe, where emulsion was produced for three days following treatment, to minor where only microscopic investigation could identify emulsions. The pH of the emulsions studied were usually in the range of 2-4. Usually, a third phase which had adsorbed to the oil-water interface was identified. The third phase was often an oil wet inorganic solid such as barite, formation material, or an asphaltene particle. They observed that solvent pre-flushes reduce the intensity of acid/crude emulsions in the formation and limit the severity of downstream emulsions.

Knopp discusses the history of acidizing-induced formation damage in Canada from the 1970's to the present from a service company perspective (Knopp 2009). In

the 1970's there was very little science or applied technology, acid-crude compatibility testing was almost never done, and "bare-bones" acid packages were pumped. He claims "bare-bones" acid stimulation often resulted in well productivity that was 10-30% of pre-stimulation drill stem test results and sometimes zero. In the 1980's Canadian producers began to realize many of the acid packages pumped created formation damage such as sludge and viscous emulsions. A major international oil company initiated a study into why acid stimulation jobs were not producing the desired results, focusing on the Goose River and Swan Hills oilfields in Alberta. It was determined the formation damage at Swan Hills was caused by a combination of asphaltic sludge and spent acid emulsion. Newly developed non-damaging acid stimulations ramped up production for the declining 30-year-old field. Today, most of the matrix and fracturing acids pumped in Canada are non-damaging, but there is potential to improve acid stimulation success in many areas of the world by minimizing formation damage such as viscous emulsion formation.

After acidizing wells in the Virginia Hill D-3 reef oil pool in Canada, several wells began producing what appeared to be a very thick emulsion. Laboratory testing showed no emulsion between the spent acid and the crude, but a black precipitate was visible at the interface of produced emulsion. The precipitate proved to have a high percentage of asphaltic material. An acid-aromatic oil emulsion was successfully used to treat wells in this formation (Moore, Crowe, and Hendrickson 1965).

Although not the focus of this investigation, emulsion upsets to surface facilities have been described by researchers (Coppel 1975; Picou, Rickets, and Luququette 1992). These problems routinely involve commingled production as a risk factor.

Partially spent acid may contain, in solution, potentially precipitable materials. As the pH of the produced acid becomes more basic after commingling with other production, fine solids capable of stabilizing extremely tight emulsions are precipitated. Although the emulsion problems may not affect well productivity, their resolution is often costly and may negate the profitability of the intended stimulation treatment.

Crude Oil Emulsion Stability

Crude oil emulsions are stabilized by films that form at the oil-water interface and inhibit the coalescence of dispersed water droplets. Heavy polar crude components including asphaltenes, resins, waxes and organic acids and bases are the primary constituents of interfacial films in crude emulsions; these heavy polar molecules are interfacially (surface) active and adsorb to the oil-water interface (Kokal 2005). In some cases, natural surfactants are produced by reactions with alkali or acidic crude components (deZabala and Radke 1986). Fine solids including clays, sand, corrosion products, mineral scales, and drilling muds may also be active at the oil-water interface; often fines are generated during acidizing operations (Kokal 2005; Krueger 1988). Interfacial films stabilize emulsions by decreasing interfacial tension and increasing interfacial viscosity (Kokal 2005). Increased interfacial film viscosity slows the rate of oil film drainage during water droplet coalescence (Jones, Neustadter, and Wittingham 1978). As a result, the rate of emulsion breakdown is greatly reduced. Demulsifiers or non-emulsifiers are designed to prevent or break up emulsions that tend to form between crude oil and live or spent acid fluids. These emulsions can be very viscous, even solid-like, and may plug the pores of the formation matrix rock (Rae and Di Lullo 2003).

Crude oil composition determines to a large extent its tendency to emulsify and the stability of emulsions formed. Aske et al. thoroughly characterized 21 different crude oils and condensates with SARA (saturates, asphaltenes, resins, aromatics) data, near-infrared spectroscopy (NIR) and physical-chemical properties. Emulsion stability for each crude was measured using an electric field technique. The emulsion stability data was correlated to the collected physical and chemical data by multivariate analysis. Asphaltene content, aggregation state of asphaltenes, and interfacial elasticity were the most important factors to high emulsion stability (Aske, Kallevik, and Sjöblom 2002).

Another study identified asphaltene content and aromatic/alkane ratio in crude oil as factors controlling emulsion stability; with increasing aromatic content emulsification tendency decreases (Eley, Hey, and Symonds 1988). Many other authors discuss the role of asphaltenes in stabilizing crude emulsions (McLean and Kilpatrick 1997; Yarranton, Hussein, and Masliyah 2000; Sztukowski, Jafari, and Alboudwarej 2002; Abdel-Raouf 2012). Alternatively, resins tend to solubilize asphaltenes in oil and remove them from the water-oil interface thus lowering emulsion stability (McLean and Kilpatrick 1997; Langevin, Poteau, Hénaut, et al. 2004; Yang, Verruto, and Kilpatrick 2007). Waxes by themselves do not stabilize emulsions, but work synergistically with asphaltenes by co-adsorbing at the interface enhancing emulsion stability (Abdel-Raouf 2012). Organic acids like naphthenic acid have also been shown to stabilize water-in-oil emulsions in some cases (Alvarado, Wang, and Moradi 2011).

Emulsion properties and stability are affected by many factors. Increased contact time between oil and water generally results in a greater resistance to interface compression and increased emulsion stability (Kimbler, Reed, and Silberberg 1966;

Jones, Neustadter, and Wittingham 1978). Dunlap and Houchin made a similar observation in their microscopic evaluation of acid return samples: what appeared to be an increasing stability of the emulsion phase with time (Dunlap and Houchin 1990). Also, temperature can affect an emulsion significantly. Temperature affects the physical properties of oil, water, interfacial films, and surfactant solubilities in the oil and water phases (Kokal 2005). Generally, with increasing temperature, emulsion viscosity and stability decrease (Jones, Neustadter, and Wittingham 1978). Droplet size and droplet size distribution affect emulsion properties as well. The droplet size distribution of an emulsion depends on interfacial tension, shear, the presence of surface active agents, and properties of the oil and water. To a certain extent, droplet size distribution determines the stability of an emulsion; in general, smaller water droplets in an emulsion correlate with longer separation time (Kokal 2005). Brine composition also has an important effect on emulsion stability. Optimum pH for water separation changes from approximately 10 for distilled water to between 6 and 7 for the bicarbonate brine solution studied by Strassner (Strassner 1968). This is due to the interaction of ions present in the brine with the asphaltenes.

Aqueous phase pH has a large impact on interfacial film stability. For most crude-brine systems and optimum pH exists where emulsion separation most readily occurs. Outside of this optimum pH range emulsion stability increases. In the case of acidizing and a low pH environment, asphaltenes may play a leading role in stabilizing emulsions as the rigid interfacial films formed by asphaltenes are strongest in acid PH (Strassner 1968; Omole and Falode 2005).

Emulsions and Sludge Formation

Emulsion stability is affected by the aggregation state of asphaltenes in the crude oil. While colloidally dispersed asphaltenes will stabilize an emulsion, there is evidence their emulsifying properties increase as they aggregate and precipitate in solid form (Kokal 2005). The aromatic portion of the asphaltene molecule can attract other aromatic groups forming nanoaggregates; nanoaggregates may associate further and create clusters (Dickie and Yen 1967; Mullins 2011). Asphaltenes are not stable in the aliphatic, non-polar part of the crude alone but are stabilized by naturally occurring resins. While asphaltenes can associate with each other in favorable conditions, in unfavorable conditions they can form larger clusters and precipitate out of the oil forming a sludge (Dickie and Yen 1967; Mullins 2011; Hashmi and Firoozabadi 2011). Unfavorable conditions can be caused by contact with aliphatic solvents, pH changes, addition of specific ions, decreasing surface tension with surfactants, temperature or pressure changes, and oxidation of asphaltenes. Once formed in the reservoir, precipitated sludge can plug formation pores, coat the formation making it oil-wet, and stabilize emulsions (O'Niel, Maley, and Lalchan 2015). While it is generally assumed sludge is always asphaltic in nature, crudes with little to no asphaltenes can produce sludge too; this is referred to as non-asphaltic sludge (Reitjens 1997).

Asphaltic sludge is insoluble in most treating chemicals and is difficult to remove once present in the formation. Jacobs described the primary factors favoring sludge formation in acidizing operations: use of hydrochloric (HCl) acid, increasing HCl acid strength, iron contaminated acid (especially the ferric Fe^{+3} ion), use of hydrochloric: hydrofluoric (HCl:HF) acid, the use of low surface tension liquids such as

diesel, and the use of some acid corrosion inhibitors (Jacobs and Thorne 1986, Jacobs 1989). On the subject of acid strength, several sources discourage the use stronger acids like 28% HCl with asphaltic crudes prone to form sludge (Mirvakili, Rohimpour, and Jahanmiri 2012; Knopp 2009). Many other design factors and fluid additives must be considered in minimizing the formation of sludge and emulsions during acid jobs: acid type, anti-sludging agents, demulsifiers, dispersants, mutual solvents, wetting agents, corrosion inhibitors, iron control additives, solvent preflush, and organic solvents (Moore, Crowe, and Hendrickson 1965; Krueger 1988; Jacobs 1989; Houchin, Dunlap, Arnold et al. 1990; O'Niel, Maley, and Lalchan 2015).

It is clear that the occurrence of viscous emulsion formation and sludge formation are closely related, often occurring in tandem. Sludge formation can block formation pores and acid/crude emulsions are often extremely viscous.

Emulsion Viscosity and Flow in Porous Media

Water-in-crude emulsions are problematic largely because of high emulsion viscosity. Emulsion viscosity can be substantially greater than the viscosity of either the oil or the water because emulsions show non-Newtonian behavior. This behavior is a result of droplet crowding or structural viscosity. Emulsion viscosity typically increases with increasing water fraction. At a certain high watercut, depending on the crude-water system, the water-in-oil emulsion will invert to an oil-in-water emulsion where the water becomes the continuous phase. This inversion is usually accompanied by a decrease in emulsion viscosity.

Emulsion flow in porous media is complex. In some cases, like when dispersed emulsion droplets are much smaller than the pore throats, treating the emulsion as a

continuous phase is adequate; characterizing continuous phase (emulsion) viscosity and assuming Darcy flow can describe the flow behavior (Alvarado and Marsden 1979). A more complex model, deep-bed filtration theory, takes into account interactions between dispersed phase emulsion droplets and the pore structure (Soo and Radke 1984a). Dispersed phase droplets may block pores with throat sizes smaller than their own, a process called straining. In a process called interception, dispersed phase droplets smaller in size than pore throats may also block flow by attaching to the surface of pore grains or in crevices. Both straining and interception result in permeability reduction. The larger the droplet, the higher the chance of capture by the media. As injection rates increase, droplets caught by straining may squeeze through the pore throat or break up through droplet snap off; droplets caught by interception may return to the emulsion flow by drop re-entrainment (Soo and Radke 1984b). If the dispersed emulsion droplets are not much smaller than the pore size, some consideration of droplet-pore structure interaction is likely necessary.

As we are studying impact of viscous acid/oil emulsions through coreflooding, we will next discuss some reports from other researchers on acidizing coreflood experiments with an emphasis on reports discussing in-situ emulsification and emulsified acids.

Laboratory Acidizing Coreflooding Experiments

Most laboratory acidizing experiments are done on brine saturated cores as it is typical to inject a brine "pre-flush" before injecting acid in the field. However, the formation rock will never be completely brine saturated. The highest possible brine saturation would be the brine saturation associated with residual oil (or gas) saturation.

Due to rock heterogeneity, relative permeability, wettability, and other factors, even with a brine pre-flush there will be a complex saturation state in the near wellbore area with brine, oil, and/or gas. Field examples of produced water-in-oil emulsions following acid stimulation have been discussed which show there will be interaction to some extent between the injected acid and the resident hydrocarbons.

Of importance to this investigation are reports of in-situ emulsification in laboratory coreflood experiments and experiments with emulsified acids. Emulsifying surfactants are sometimes used to disperse acid in a continuous oil phase. The oil phase is typically a produced crude or refined hydrocarbon (Buijse and van Domelen 1998). This fluid system is referred to an emulsified acid and is designed to delay the reaction between the acid and rock. These systems are more commonly used in acid fracturing where it is desirable to delay the spending of acid to maximize the length of the etched fracture face; use of emulsified acids is less frequent in matrix acidizing (Rae and Di Lullo 2003).

Some authors have, however, reported on the benefits of emulsified acids in matrix acidizing. Bazin and Abdulahad showed in coreflood experiments that use of emulsified acids created deeper penetrating wormholes at low flow rates whereas plain HCl tended to create a face dissolution pattern at the same injection rates. From this the authors suggest emulsified acids may have application in low-permeability reservoirs (Bazin and Abdulahad 1999).

Another coreflood study showed that emulsified acids may provide better wellbore coverage and create deeper wormholes at low injection rates in heterogeneous reservoirs (Buijse and van Domelen 1998). The authors also describe differences in

wormhole characteristics and injection pressure response between emulsified acid and plain acid: emulsified acids tended to create many very narrow wormholes through the core. At breakthrough a slow drop in pressure was noted but the pressure did not drop to zero immediately. This is because the fluid friction in the narrow channels was still high at breakthrough and the width of the channels increased slowly due to the retardation of the acid. With plain HCl, wider wormholes were created in cores and a sharp drop in injection pressure to zero was noted at breakthrough.

Al-mutairi et al. performed coreflood experiments in fluid saturated cores with different grade oils (Al-mutairi, Al-Obied, Al-Yami et al. 2012). Corefloods were performed on cores saturated with tar, intermediate oil (32°API), and condensate oil (45°API) using regular HCl and Emulsified HCl. Cores with heavier °API oil were found to have a low acid breakthrough volume. The authors theorize the in-situ emulsification process and generation of stable acid-in-oil emulsion helped form deeper wormholes. They also note the benefit from emulsified acid diminished when rocks were saturated with oil; they attribute this to acid-oil emulsification that provides a similar magnitude of retardation. Using regular acid created multiple wormholes when heavier oil was used but not in condensate saturated cores; they again theorize regular HCl effectively emulsifies with the heavier oils but not the condensate.

Sayed et al. studied the effect of oil saturation on acidizing with emulsified acids (Sayed, Assem, and Nasr-El-Din 2014). They found the volume of emulsified acid to achieve breakthrough in cores saturated with a crude oil was greater by 2 to 2.5 times that needed for cores fully saturated with water. In cores saturated with crude at irreducible water saturation, the volume of emulsified acid to achieve breakthrough was

1.3 to 2.0 times greater than that needed for cores fully saturated with water. The authors also not the lack of an optimum injection rate for the range of emulsified-acid injection rates studied.

To the best of our knowledge there is only one publication by Al-mutairi et al. proposing in-situ acid/crude emulsification to explain acidizing coreflood results (Al-mutairi, Al-Obied, Al-Yami et al. 2012). Their proposal is logical but remains unsubstantiated by direct experimental evidence.

Objectives

The objectives of this study are (1) to study the effect of acid volume fraction on acid-in-crude emulsion viscosity and stability with bottle testing and (2) investigate the in-situ formation of acid-in-crude emulsions in crude saturated carbonate cores during matrix acidizing. Some coreflooding tests will aim to quantify the impact of in-situ emulsification on a following oil injection period.

CHAPTER 2: EXPERIMENTAL METHODOLODY

Two types of experiments were performed in this study: emulsion bottle testing and coreflooding. This section contains a description of the experimental fluids, rocks, apparatus, and procedures.

2.1 Fluids

- 15% hydrochloric acid (HCl) by weight was used in bottle testing and coreflooding experiments. It was diluted from 37% HCl (wt.) with deionized water. The dilution factor used and its derivation are shown below:

$$15\%\ HCl\ (wt) = \frac{1.467\ g\ \ DI\ water}{g\ 37\%\ HCl\ (wt)}$$

$$100g\ 37\%\ HCl = \ 37g\ HCl\ and\ 63\ g\ water$$

$$15\%\ HCl\ with\ 37g\ HCl\ requires\ 209.7\ g\ water$$

$$209.7 - 63 = 146.7\ g\ water\ added\ to\ 100\ g\ 37\%\ HCl\ or\ \frac{1.467\ g\ water}{g\ 37\%\ HCl\ (wt)}$$

- Deionized water was used to dilute the HCl and to saturate some cores. It was injected through the coreflooding setup after a test for cleaning.
- Dead crude oil, produced in North Texas, was used in bottle testing and coreflooding experiments. It was purchased from www.RawCrudeOil.com. The properties of the oil are shown in **Table 1**.

Table 1: Physical Properties of Crude Oil

Density (g/cc)	Viscosity (cp)
0.88	25.6 ± 0.6

- Mineral oil was used in coreflooding experiments. Its properties are shown in **Table 2**.

Table 2: Physical properties of Mineral Oil

Density (g/cc)	Viscosity (cp)
0.87	32.4

- Toluene was used to clean capillary viscometers and glassware.
- Acetone was used to clean capillary viscometer and glassware.
- Nitrogen gas was used to apply back pressure in some coreflood experiments

2.2 Rock Samples

Cores were cut with 1.5" diameter and 6" length from limestone blocks with permeability ranging 2 – 4 mD. The limestone blocks were purchased from Kokurek Industries, TX.

2.2a Cutting Cores

A 1.5" x 8" coring bit is used on a large drilling machine to cut the cores. The limestone block is placed on 2" x 4" wood planks and secured into place with the machine clamps. If the block is not sufficiently level, the wood planks and block are rearranged to correct this. An automatic bit feeding mode is used on the machine to lower the drill bit at a constant rate; this helps cut cores with a smooth outer surface and constant diameter. Water is used as the coring fluid to keep the bit cool and remove the cuttings.

2.2b Core Preparation

Core ends are polished with sandpaper when they are not perpendicular to the core axis or when they are not flat or are chipped. Cores are dried in an oven for 24 hours at 100 °C and then removed and allowed to cool overnight.

2.2c Core Porosity Measurement

Core length, diameter, and dry mass are each measured five times and averaged. Bulk volume of the core, V_B, is calculated as:

$$V_B = \frac{\pi D^2 L}{4} \qquad where\ L = length\ and\ D = diameter$$

Grain volume of the core, V_G, is calculated assuming the grain density is equal to that of calcite:

$$V_G = \frac{core\ mass, g}{2.71\ g/cc}$$

Pore volume of the core, V_P, is defined as:

$$V_P = V_B - V_G$$

Finally, core porosity, Φ, is defined as:

$$\Phi = \frac{V_P}{V_B}$$

2.2d Core Saturation

Some cores are left unsaturated but most cores are saturated with either crude, deionized water, or mineral oil. The saturation setup during is shown in **Figure 1** during the vacuuming step. A saturation flask is connected to a valve system which is connected to the cold trap and vacuum pump.

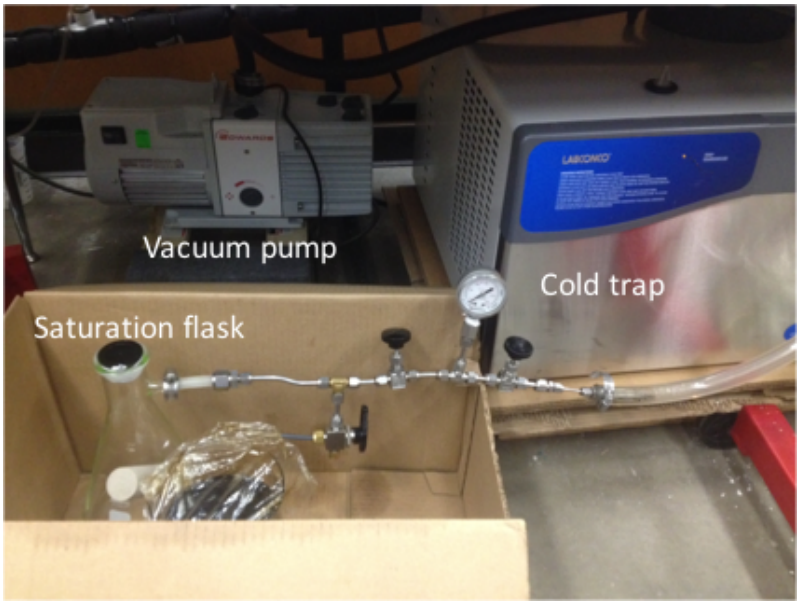

Figure 1: Core Saturation Apparatus

The steps for core saturation are listed:

1. Turn the cold trap on 30 minutes to 1 hour ahead of time. Ensure tight tubing connections between the vacuum pump and the cold trap and between the cold trap and the valve system.
2. Place the core in the clean, dry saturation flask careful not to cause damage. By turning the saturation flask upside down, inserting the core, and slowly turning the flask right-side up, damage is avoided.
3. Connect the plastic tubing on the valve system to the saturation flask and tighten the metal clamp around the connection.
4. Insert the rubber stopper, wrapped with Teflon if necessary, into the saturation flask. It should seal very tightly to avoid leaks.
5. Fill a large beaker with about 2 liters of the saturating fluid and place the fill line on the valve system in the beaker so that it is touching the glass base. Make sure the valve on fill line is closed.
6. Make sure both needle valves on the valve system are open and turn on the vacuum pump.
7. Quickly open and close the valve on the fill line to fill the line with fluid.
8. Vacuum for 2 hours. Typically, a reading of -25 psi shows on the gauge.
9. Close the needle valve to the right of the pressure gauge and open the fill line valve. Fluid will quickly fill the saturation flask if there are no major leaks. When the core is fully submerged, close the fill line valve.
10. Turn off vacuum pump and cold trap. Allow submerged core to sit for 24 hours under vacuum.

11. Disassemble the saturation flask and submerge the core in the saturating fluid in a container to age. Starting with core LS-7 the goal was to age cores for 14 days, but there are some deviations due to equipment access and maintenance.

An unsaturated core and a crude-saturated core are pictured in **Figure 2**.

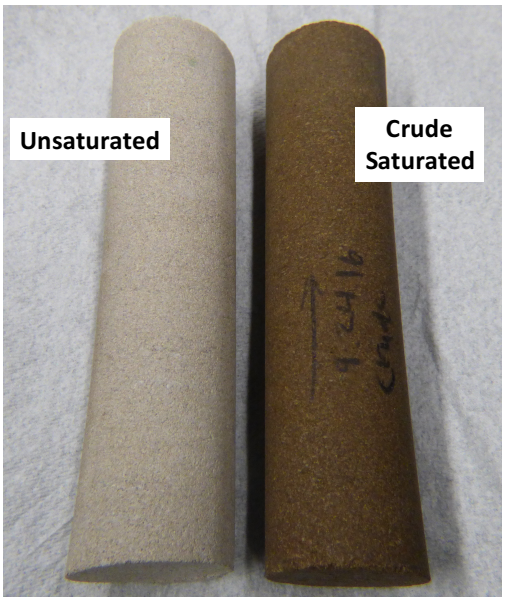

Figure 2: Unsaturated and Crude-saturated Cores

2.2e Core Saturation Measurement

Excess fluid is wiped off the sides of the saturated core with a latex glove and the core is weighed. The fluid volume in the core, V_F, is defined as:

$$V_F = \frac{saturated\ mass - dry\ mass}{fluid\ density}$$

The fluid saturation of the core, expressed as a percentage, is defined as:

$$Saturation = \frac{V_F}{V_P}$$

2.2f Core Characteristics

The cores have an average porosity of 16.5%. Cores LS-2 through LS-5 were cut from the same limestone block and have porosities ranging from 15.7% to 16.0%. Cores LS-7 through LS-15 were cut from another limestone block and have porosities ranging from 16.6% to 17.0%. Fluid saturations range from 95% to 98% indicating good core saturation. With the exception of cores LS-4 and LS-9 all cores are aged at least 14 days. The relevant data for each core is shown in **Table 3**.

Table 3: Core Parameters

Core	Dimensions (cm)		V_P (cc)	Φ (%)	Aging (days)	Saturation (%)		
	L	D				Crude	Min. Oil	DI water
LS-2	15.44	3.79	27.4	15.8	60	98		
LS-3	15.29	3.76	26.6	15.7	-			
LS-4	15.31	3.76	26.7	15.7	2	97		
LS-5	15.37	3.76	27.3	16.0	-			
LS-7	15.39	3.78	28.6	16.6	19	97		
LS-8	15.32	3.78	29.1	16.9	15			95
LS-9	15.41	3.78	29.0	16.8	4	97		
LS-10	15.59	3.77	29.4	16.9	31		97	
LS-11	15.43	3.78	29.2	16.9	16	96		
LS-12	15.16	3.78	28.9	17.0	14	98		
LS-13	15.26	3.78	28.9	16.9	14	97		
LS-14	15.17	3.78	28.8	16.9	14		97	
LS-15	15.06	3.78	28.0	16.6	16	99		

2.3 Emulsion Bottle Testing

An emulsion bottle test is a common test in which two immiscible phases (like oil and water) are mixed in a container to study the emulsifying properties of the mixture. Bottle tests in this study involve mixtures of 15% HCl (wt.) and crude oil to study the effects of acid volume fraction and separation time on emulsion viscosity and stability.

2.3a Experimental Setup

The model T18 homogenizer manufactured by IKA is used to mix emulsions. The homogenizer and an emulsion being mixed are shown in **Figure 3.** Plastic graduated vials (15cc and 50cc) are used to divide emulsions into 10 portions immediately after mixing, shown in **Figure 4**.

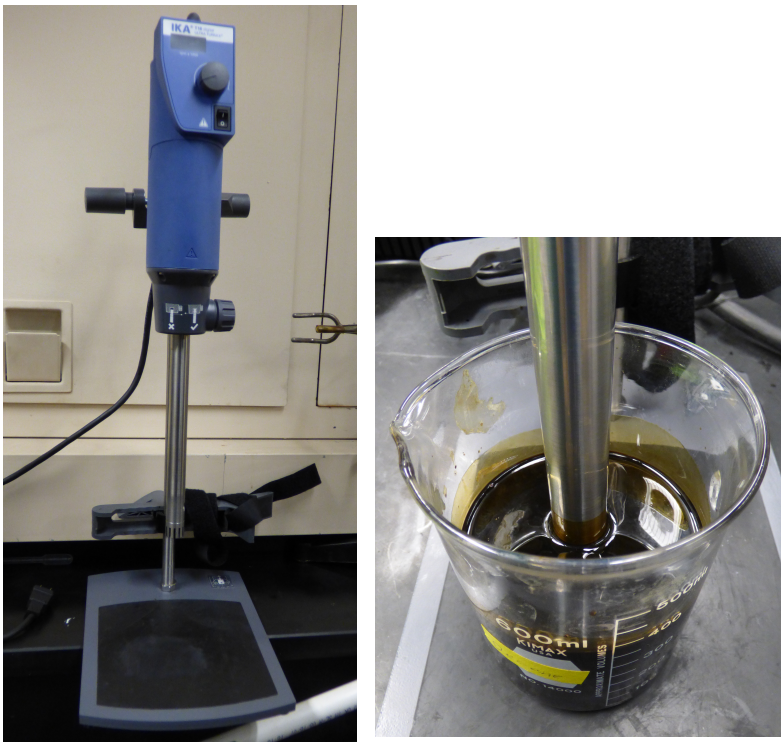

(a) (b)

Figure 3: (a) IKA T18 Homogenizer (b) Mixing Emulsion

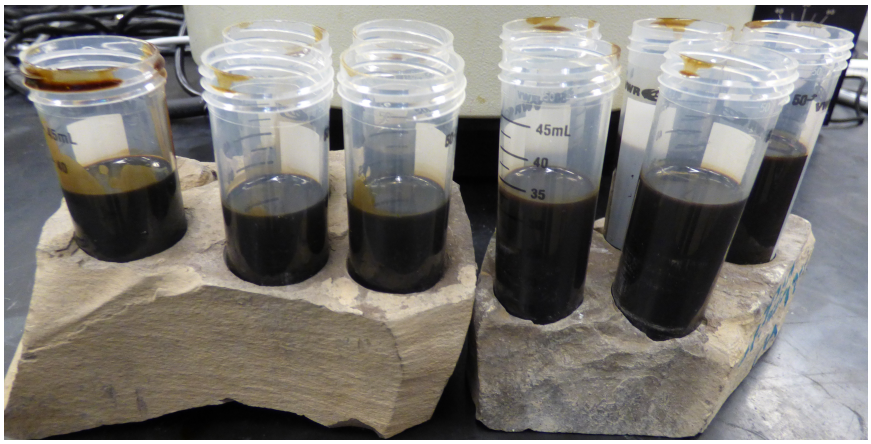

Figure 4: Emulsion Poured into Graduated Vials

Cannon capillary viscometers, shown in **Figure 5**, are used for all viscosity measurements. Emulsion properties change with applied shear and a capillary viscometer does not shear the emulsion like other rotational viscometers. For the emulsions studied, the most viscous portion tends to separate to the bottom of each vial with time. For this reason, emulsion is extracted from the bottom of each vial with a pipette for measurement as seen in **Figure 6**.

(a) (b)

Figure 5: (a) Cannon Viscometer (b) Measuring Viscosity

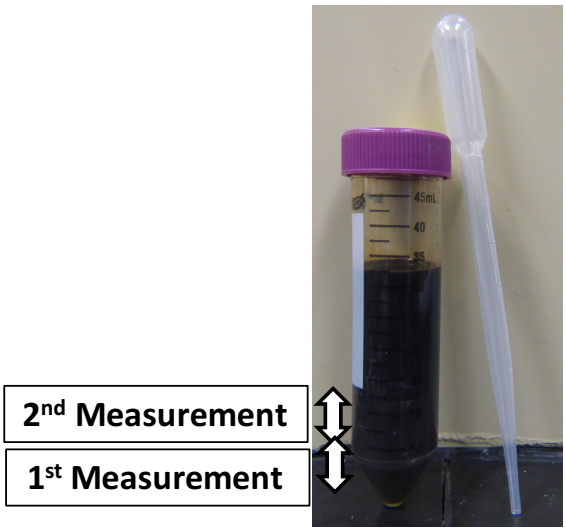

Figure 6: Emulsion Fluid Measured in Each Vial

Emulsion density is measured by pouring fluid from the viscometer into a 15cc graduated vial so that the fluid aligns with a graduation. This is shown in **Figure 7**. The fluid is weighed and its mass and volume are recorded.

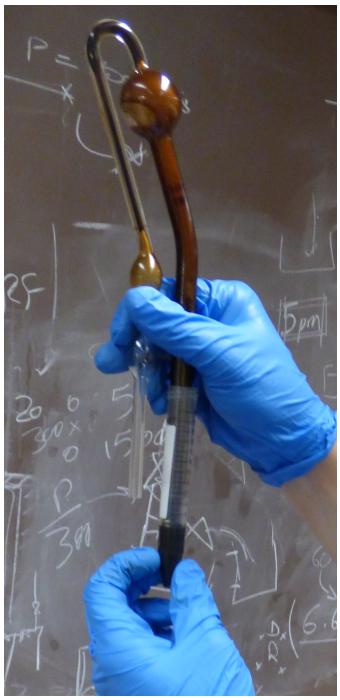

Figure 7: Transferring Emulsion for Density Measurement

2.3b Procedure

Four sets of emulsions with acid volume fractions ranging from 20%-40% were studied as shown in **Table 4**. After integrating experience from studying Emulsion 1 it was decided to increase the total volume and individual vial volumes for Emulsions 2 – 4.

Table 4: Summary of Mixed Emulsions

Emulsion	Vol. % Acid	Vol. % Crude	Total Volume (ml)	Vial Emulsion Volume (ml)
1	30.0	70.0	200.0	15
2	30.0	70.0	339.9	32
3	20.0	80.0	340.0	32
4	40.1	59.9	339.4	32

Aspects of the emulsion bottle testing procedure are credited to Oluwatosin (Oluwatosin 2016). The procedure is listed:

1. Convert desired acid and crude volumes for a given emulsion to mass based on fluid densities.
2. Weigh crude and acid in a beaker and record actual weights. The total fluid level must be sufficient to submerge the homogenizer; 300 ml beaker used for Emulsion 1, 600 ml beaker used for Emulsions 2 – 4.
3. Arrange the homogenizer tip in the center of the beaker approximately 1 cm from the bottom and mix at 5000 rpm for 30 minutes.
4. Pour the mixed emulsion in 10 x 15 ml vials, 15 ml fluid each (Emulsion 1) or 10 x 50 ml vials, 32 ml fluid each (Emulsions 2-4).
5. At t = 0 hours, 1 hour, 2 hours, 5 hours, 1 day, 2 days, 3 days, 4 days, and 5 days measure viscosity and density twice from a vial: first by sampling the bottom-most fluid and second by sampling the next bottom-most fluid. Record observations on separation.
    a. Viscosity: Fill the bulb on the viscometer about halfway using a pipette to extract emulsion from the vial. Use the suction to draw the fluid up through the capillary above the top marked line. Remove the suction and start the timer when the fluid has dropped to the top line. Stop the timer when the fluid reaches the bottom line. Multiply efflux time by the viscometer constant to obtain kinematic viscosity. Multiply kinematic viscosity by density to obtain dynamic viscosity.
        i. Size 300 viscometer (50 – 250 cSt range) for Emulsions 1-3.

ii. Size 400 viscometer (240-1200 cSt range) for Emulsion 4

b. Density: Tare the scale with an empty 15 cc graduated vial and stand. Pour the emulsion from the viscometer into the vial (by inserting the viscometer into the vial you can avoid getting fluid on the upper sides of the vial)

c. Stability: Observing or photographing any phase separation is hard because the oil and emulsion are nearly the same color. With the spare vial, you can tilt it on the side to see if a more viscous portion has separated out. This fluid will be very slow to pour and quasi-solid.

6. Rinse capillary viscometers with toluene followed by acetone followed by air.

2.4 Coreflooding

Coreflooding is a common experiment in petroleum engineering. Confining pressure is applied around a cylindrical rock sample and fluid flows through the core when a pressure gradient is applied. A coreflooding apparatus was assembled to study the in-situ formation of acid-in-crude emulsions and effects of the emulsions on oil production. The apparatus was configured for three types of experiments:

- full wormhole propagation (no backpressure)
- full wormhole propagation (1200 psi backpressure)
- partial wormhole propagation and oil injection

2.4a Experimental Setup – Full Wormhole Propagation (no backpressure)

The experimental setup for full wormhole propagation with no backpressure is diagramed in **Figure 8**. The setup includes a Hassler type coreholder that is connected to an accumulator and pressure transducer at the inlet. A hydraulic confinement pump applies overburden pressure with mineral oil on a rubber sleeve in the coreholder. The core fits in the rubber sleeve. Acid is injected from the accumulator through the core using an ISCO syringe pump. Effluent fluid is collected at the coreholder outlet in glass vials. During injection the inlet pressure is read from the pressure transducer display and recorded.

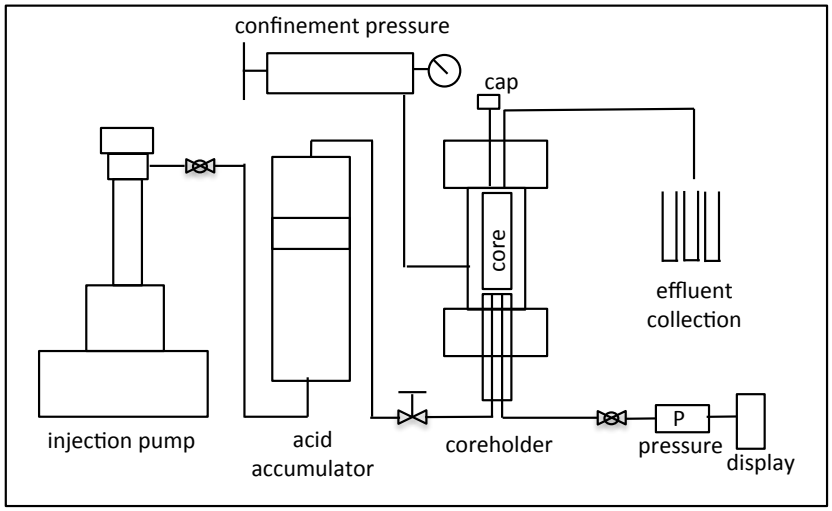

Figure 8: Setup for Full Wormhole Propagation (no backpressure)

2.4b Procedure – Full Wormhole Propagation (no backpressure)

The procedure for the full wormhole propagation (no backpressure) experiment is listed:

1. Fill one line on the core inlet plug with mineral oil and connect the pressure transducer.
2. Inject acid through the other inlet line to the inlet plug face.
3. Pack core in the coreholder and apply 1500 psi overburden pressure.

4. Inject acid at 3.5 cc/min and record pressure every 15 seconds.
5. When injection pressure drops to 0 record the breakthrough time. Test collected effluent for pH and also viscosity for the crude-saturated core.
6. Stop acid injection, release overburden, and remove core.
7. Flush metal tubing and coreholder with deionized water.

2.4c Experimental Setup – Full Wormhole Propagation (1200 psi backpressure)

The experimental setup for full wormhole propagation (1200 psi backpressure) is diagramed in **Figure 9**. The setup is the same as the one for full wormhole propagation (no backpressure) with a few additions:

- The coreholder outlet is connected to an effluent accumulator and nitrogen gas tank. The effluent accumulator is connected to another ISCO syringe pump.
- A data acquisition unit is connected to the pressure transducer to record pressure starting with core LS-7. The data acquisition setup is shown in **Figure 10.**

Backpressure of 1200 psi is applied to the core to keep as much CO_2 generated from the reaction between the acid and the rock in liquid form. Pressure is applied with nitrogen gas from the tank and then the backpressure syringe pump is run at a 1200 psi constant pressure during the experiment. Acid is injected through the core and at breakthrough effluent fluid in collected in the effluent accumulator.

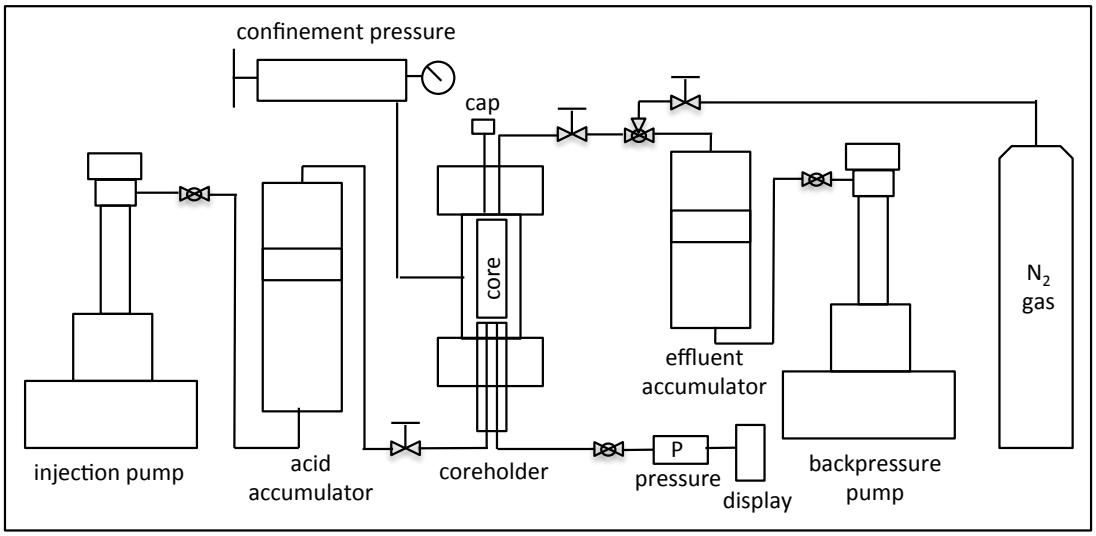

Figure 9: Setup for Full Wormhole Propagation (1200 psi backpressure)

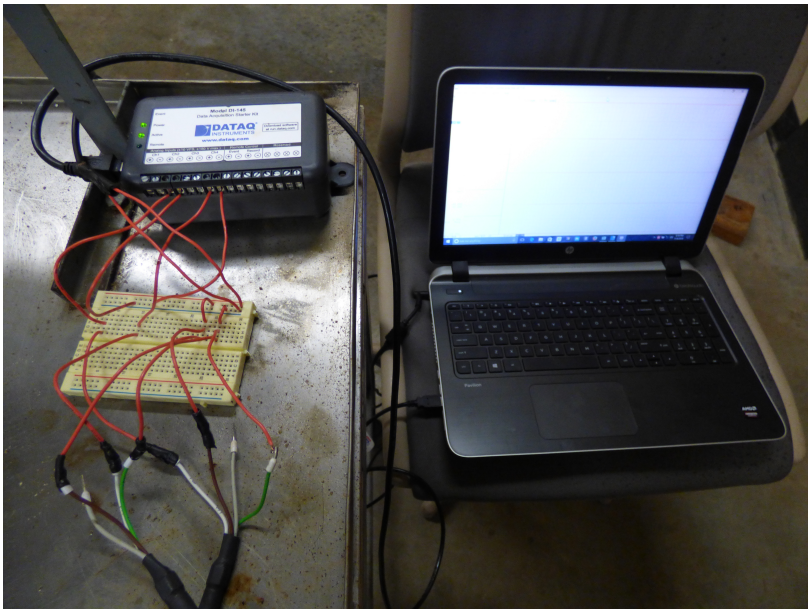

Figure 10: Data Acquisition Setup

2.4d Procedure – Full Wormhole Propagation (1200 psi backpressure)

The procedure for the full wormhole propagation (no backpressure) experiment is listed:

1. Fill one line on the core inlet plug with mineral oil and connect the pressure transducer.

2. Inject acid through the other inlet line to the inlet plug face. Close the needle valve on this inlet line.
3. Pack core in the coreholder and apply 2500 psi overburden pressure.
4. Apply 1200 psi pressure using the nitrogen gas tank and then close the valve on this line. Run backpressure pump run at 1200 psi constant pressure.
5. Run the inlet pump at 1200 psi constant pressure.
6. Open the valve on the inlet line.
7. Injected acid at 3.5 cc/min and record pressure every 15 seconds. Pressure is recorded by computer for experiments utilizing data acquisition.
8. When injection pressure drops to 0 record the breakthrough time. Continue to collect effluent fluid for 1.5 min after breakthrough.
9. Stop acid injection and close valve on inlet line.
10. Refill the backpressure pump completely to lower system pressure and then bleed remaining pressure from needle valve on outlet line.
11. Reduce the injection pump pressure to 0 psi.
12. Release overburden, remove core, and flush metal tubing and coreholder with deionized water.
13. Record observations on fluid in effluent accumulator.

2.4e Experimental Setup –Partial Wormhole Propagation and Oil Injection

The experimental setup for partial wormhole propagation and oil injection is diagramed in **Figure 11** and pictured in **Figure 12**. The setup is the same as the one for full wormhole propagation (1200 psi backpressure) except a pressure transducer is connected to the outlet line instead of the nitrogen gas tank and the oil accumulator and

outlet lines are filled with oil. Acid is injected into the core for 1 or 1.5 minutes so that a wormhole is does not fully propagate and then oil (crude or mineral oil) is injected at constant rate from the outlet.

Experiments are performed on cores saturated with crude oil and cores saturated with mineral oil. From simple bottle tests we know the acid does not form an emulsion with mineral oil, so if the in-situ formation of acid-in-crude emulsions impedes flow during crude oil injection, we should be able to observe a higher oil injection pressure with the crude-saturated cores.

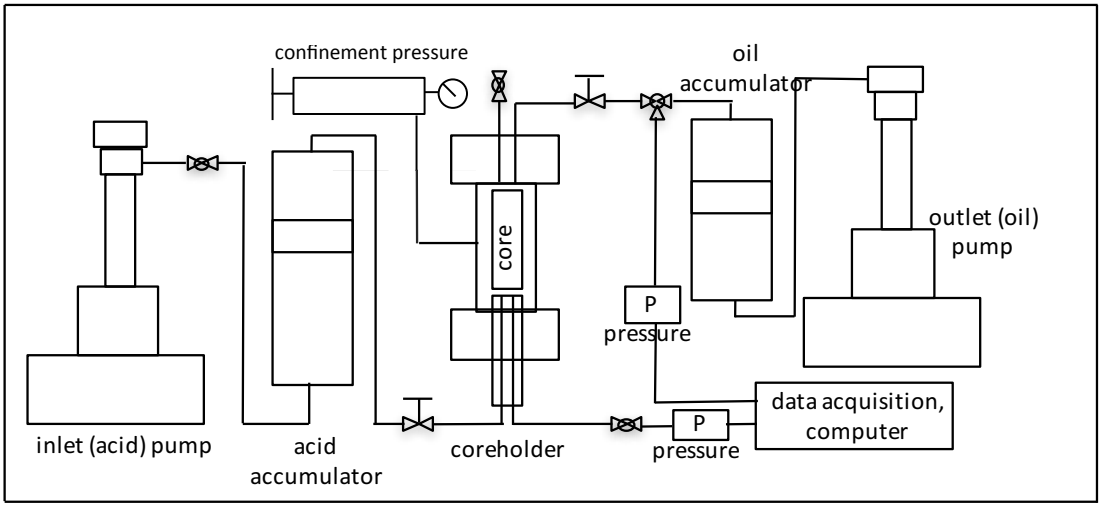

Figure 11: Setup for Partial Wormhole Propagation and Oil Injection

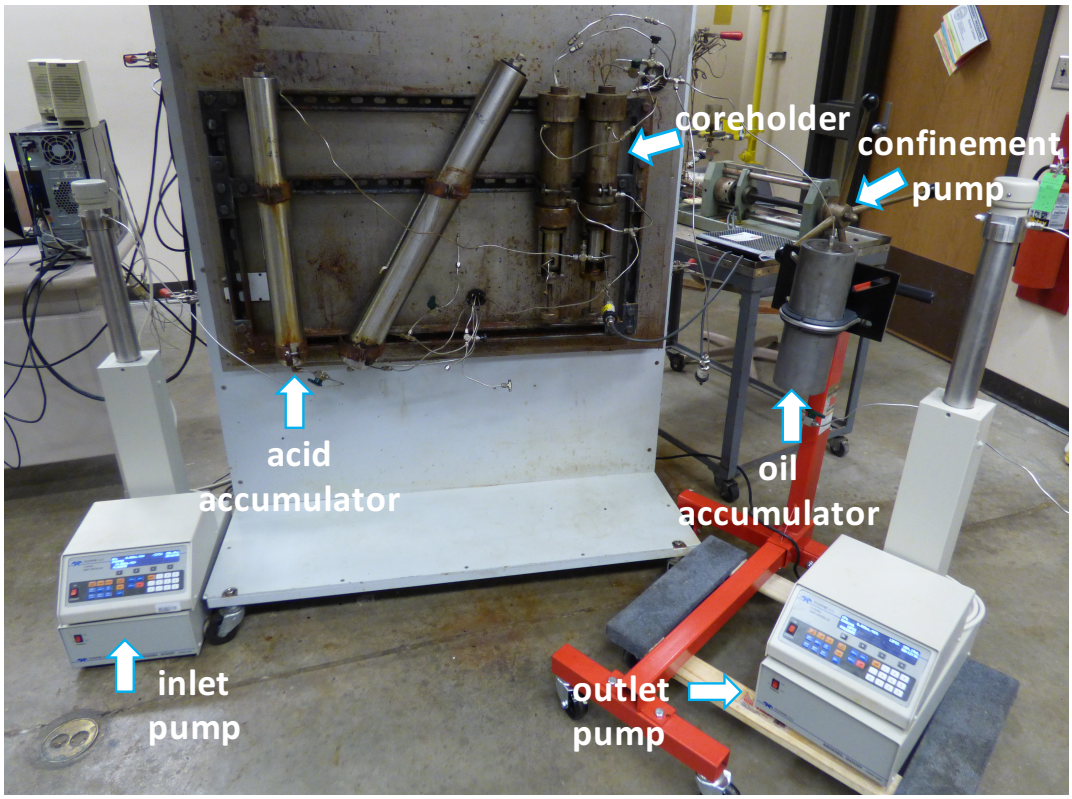

Figure 12: Setup for Partial Wormhole Propagation and Oil Injection (Picture)

2.4f Procedure – Partial Wormhole Propagation and Oil Injection

The procedure for the partial wormhole propagation and oil injection experiment is listed:

1. Fill all coreholder outlet lines with oil and connect the outlet pressure transducer and oil accumulator.
2. Pack core in coreholder and apply 2000 psi overburden.
3. Inject oil from the outlet, through to core, to fill both lines on the inlet plug with oil. Connect the inlet pressure transducer.
4. Run the outlet pump at constant rate to inject 50 cc of oil through core (initially 0.5 cc/min, but lowered to 0.3 cc/min in subsequent experiments). This step is not completed for core LS-9 or LS-15.

5. Close the needle valve on the inlet line.
6. Inject acid to fill the line connected to the accumulator and then connect this line to the valve on the inlet line. (The dead volume from the valve to the inlet plug face is 0.7 ml)
7. Increase overburden to 3200 psi.
8. Run the outlet pump at 1200 psi constant pressure.
9. Run the inlet pump at 1200 psi constant pressure.
10. Open the inlet line valve and inject acid at 3.5 cc/min for 1 minute. Core LS-15 has an acid injection period of 1.5 minutes.
11. Stop injection at inlet pump and run pump at 1200 psi constant pressure.
12. For cores LS-12 and LS-15, close the inlet line valve and wait 24 hours before proceeding.
13. Run the outlet pump at a constant rate to inject 50 cc of oil through core (initially 0.5 cc/min, but lowered to 0.3 cc/min in subsequent experiments.
14. Stop injection at the outlet pump and reduce pump pressure to 1200 psi.
15. Reduce inlet pump pressure to 0 psi and outlet pump pressure to 0 psi.
16. Release overburden, remove core, and flush metal tubing and coreholder with deionized water.

CHAPTER 3: EXPERIMENTAL RESULTS AND DISCUSSION

The experimental work is divided into two main types of experiments: emulsion bottle tests for viscosity and stability and acid coreflooding experiments.

3.1 Emulsion Bottle Testing

In order to investigate the effect of acid fraction and settling time on emulsion viscosity and stability, acid in crude emulsions were prepared with different volume fractions of acid (15% HCl by vol.). Measurements of viscosity and density were made at specific time intervals (0 hours, 1 hour, 2 hours, 5 hours, 1 day, 2 days, 3 days, 4 days, 5 days) and notes on emulsion stability were taken. At each time interval for each emulsion two measurements were typically taken: the first testing the bottom-most fluid in the vial and the second testing the next bottom-most fluid in the vial.

3.1a Emulsion Separation and Stability vs. Time

All four emulsions have similar separation characteristics. The main observation with respect to fluid separation is a highly viscous acid-in-oil emulsion that separates at the bottom of each vial with less viscous emulsion and/or free oil on top. This usually happens between 5 hours and 24 hours after mixing. Separation of Emulsion 4 (40% acid vol.) is shown in **Figure 13**: immediately after mixing the fluid in the vial is semi-continuous and it flattens out when the vial is tilted on its side. At 2 days and later, however, the viscous portion in the bottom is very slow to pour once the vial is tilted on its side.

There is also free acid that is observed when making some of the viscosity measurements, but it is always a very small volume. The majority of the acid stays

emulsified in the oil. Aside from the separation described, the tight emulsion that separates to the bottom of the vial is stable indefinitely.

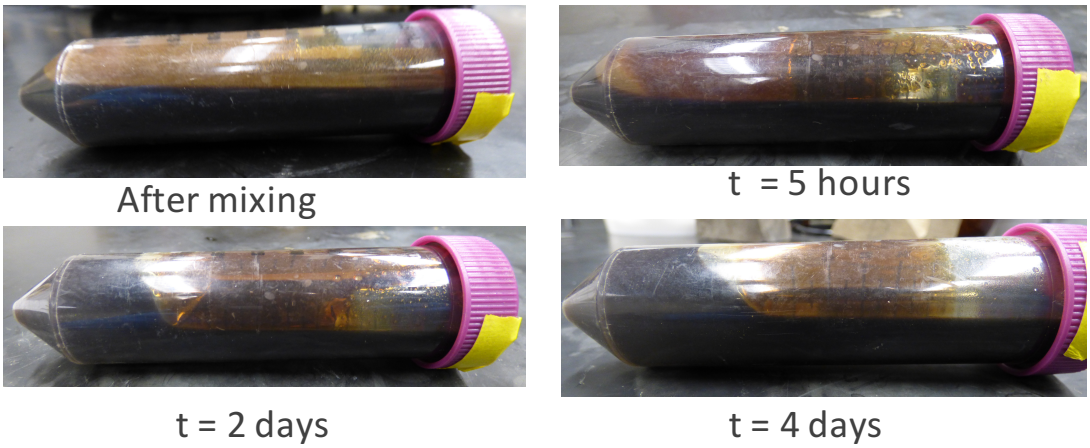

Figure 13: Emulsion 4 (40% Acid) Separation vs. Time

3.1b Emulsion Viscosity vs. Time and Initial Acid Fraction

Viscosity of the prepared emulsions tends to increase dramatically with time. This is due to the separation of the higher acid-fraction emulsion as described. Less viscous, lower acid-fraction emulsion and/or free oil tend to separate toward the top of the vial. After mixing, viscosity is roughly equivalent between the bottom-most fluid and the next bottom-most fluid for each emulsion as shown in **Table 5**. Given time to separate though, the maximum measured viscosities are much higher for the bottom-most fluid compared to the next bottom-most fluid. Also, emulsion viscosity increases with increasing acid volume fraction. We might expect Emulsions 1 and 2 to have more equivalent viscosities right after mixing, but they were mixed in different size beakers due to differences in total volume. Emulsion 1 was mixed in a smaller beaker with a higher fluid level which likely resulted in more efficient mixing.

Table 5: Summary of Emulsion Viscosity

Emulsion	Vol. % Acid	Vial Volume (ml)	Bottom-most Fluid Viscosity (cP)		Next Bottom-most Fluid Viscosity (cP)	
			After mixing	Maximum measured	After mixing	Maximum measured
1	30.0	15	136	224	128	205
2	30.0	32	106	888	103	165
3	20.0	32	46	383	46	105
4	40.1	32	147	3187	146	343

As seen in **Figure 14**, the viscosity measurements for Emulsion 1 group tightly together at 0 hours, 1 hour, and 2 hours between 125 cP and 150 cP; however, after these early times, some viscosity measurements near or above 200 cP are made. The most viscous fraction that separates to the bottom of each vial is only about 4cc which is not enough to measure properly with the capillary viscometer. For this reason, Emulsions 2 – 4 were mixed so that a greater volume could be put in each vial.

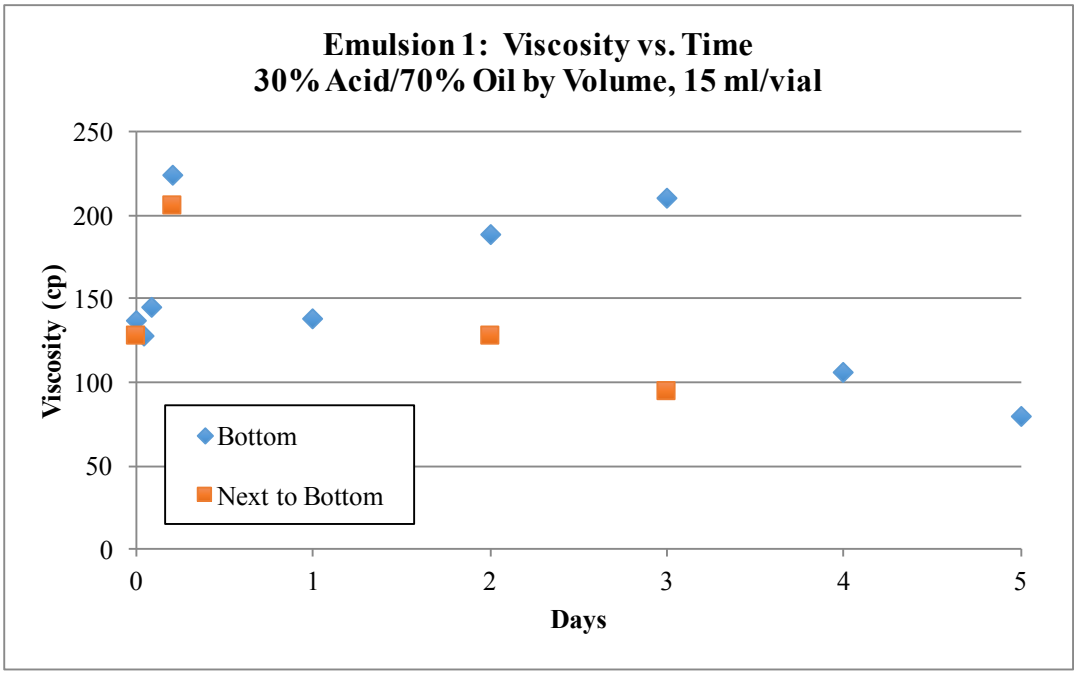

Figure 14: Emulsion 1 Viscosity vs. Time

Compared to Emulsion 1, larger values for viscosity are measured with Emulsion 2 because there is adequate fluid for measuring the most viscous, separated fraction as shown in **Figure 15**. Several viscosity measurements are in the 400 – 900 cP range. Viscosity measurements of the bottom-most vial fluid were not completed on days 4 and 5 since this fluid blocked the capillary viscometer and became stuck, but qualitatively we can be sure it isvery viscous. Similar to Emulsion 1, a small difference is seen between the bottom-most fluid and the next bottom-most fluid measurements at early times, but at 1 day and later, the viscosity difference is large as fluid separation has occurred.

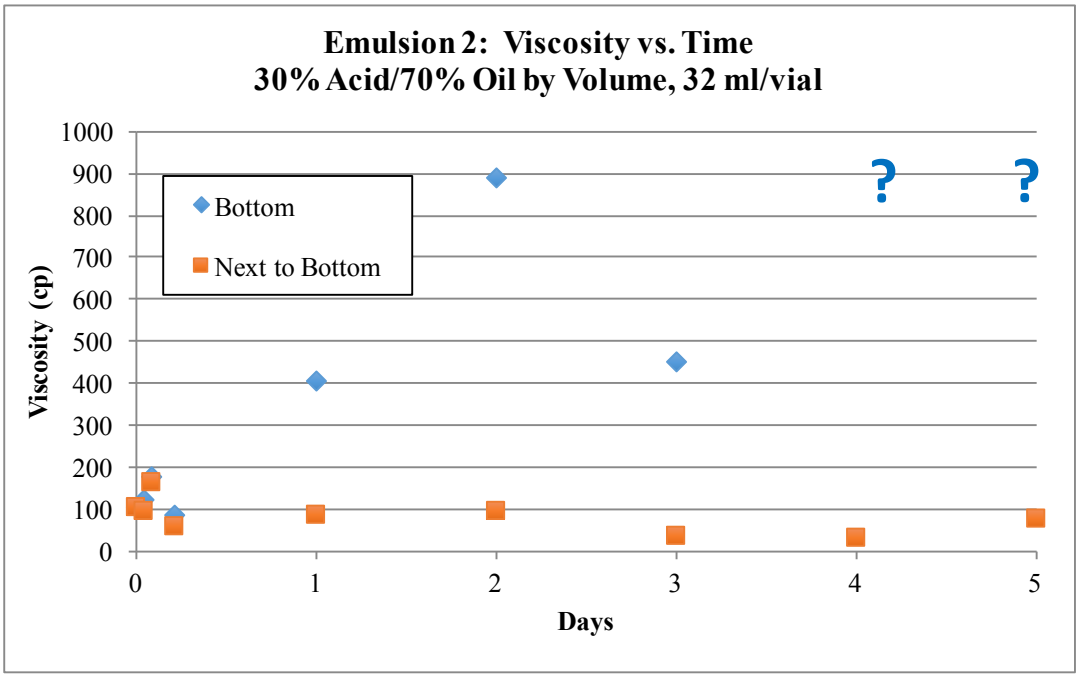

Figure 15: Emulsion 2 Viscosity vs. Time
? –emulsion clogged viscometer during measurement

Emulsion 3, 20% acid by volume, has the lowest acid fraction of all emulsions tested. As expected, measured viscosities for this emulsion, shown in **Figure 16**, are on average lower than the other emulsion. However, some viscosity measurements between 200 - 400 cP are eventually made due to separation and a higher than initial acid fraction in the most viscous portion.

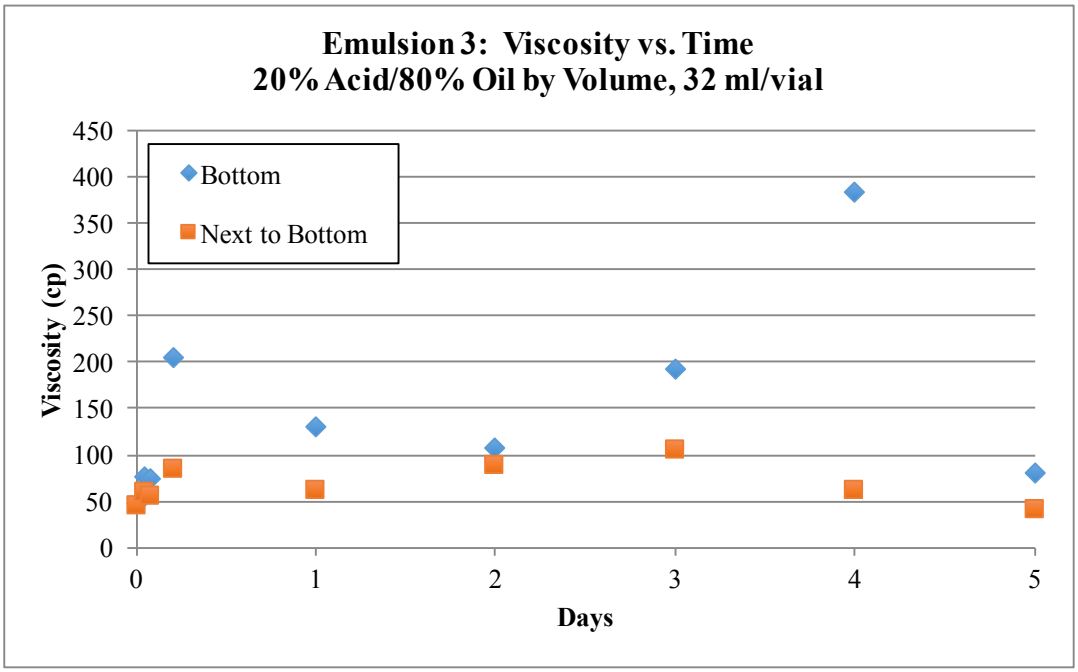

Figure 16: Emulsion 3 Viscosity vs. Time

Emulsion 4 has the greatest initial acid fraction, 40%. The highest viscosity measurement in this study, up to 3000 cP, are made on this emulsion, as shown in **Figure 17**. Like the previous emulsions, early viscosity measurements at 0 hours, 1 hour, and 2 hours all measure within a fairly close range of 100-200 cp, but at later times there are much larger differences between the bottom-most and next bottom-most fluid viscosities.

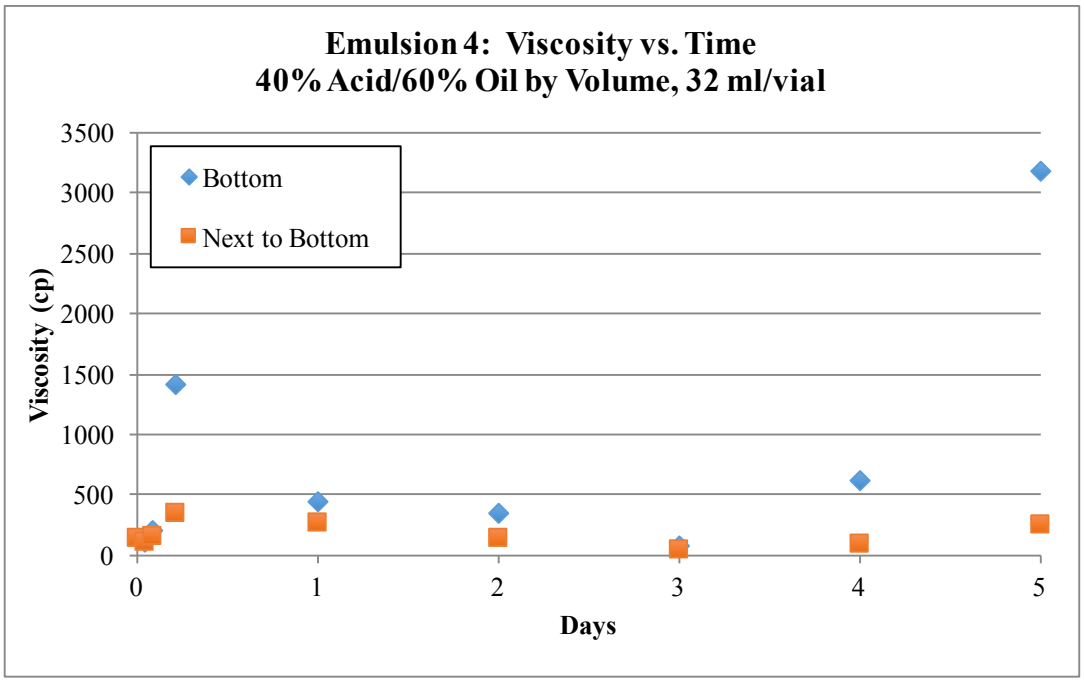

Figure 17: Emulsion 4 Viscosity vs. Time

3.1c Emulsion Viscosity vs. Density

As shown in **Figures 1 – 4**, measured emulsion viscosities are not very consistent and sometimes span a large range for the same emulsion. This is partly because the distribution of fluid in each vial changes over time. Also, it is very difficult to perfectly standardize the extraction of fluid via pipette. Most of the variation in viscosity measurements can be explained by the variation in acid volume fraction of the extracted fluid. This is shown in the correlation between emulsion viscosity and density (a proxy for acid fraction) in **Figure 18** and **Figure 19**. Emulsion density increases with acid fraction due to density differences between the acid and the crude. Higher emulsion viscosity is correlated with higher emulsion density and vice versa.

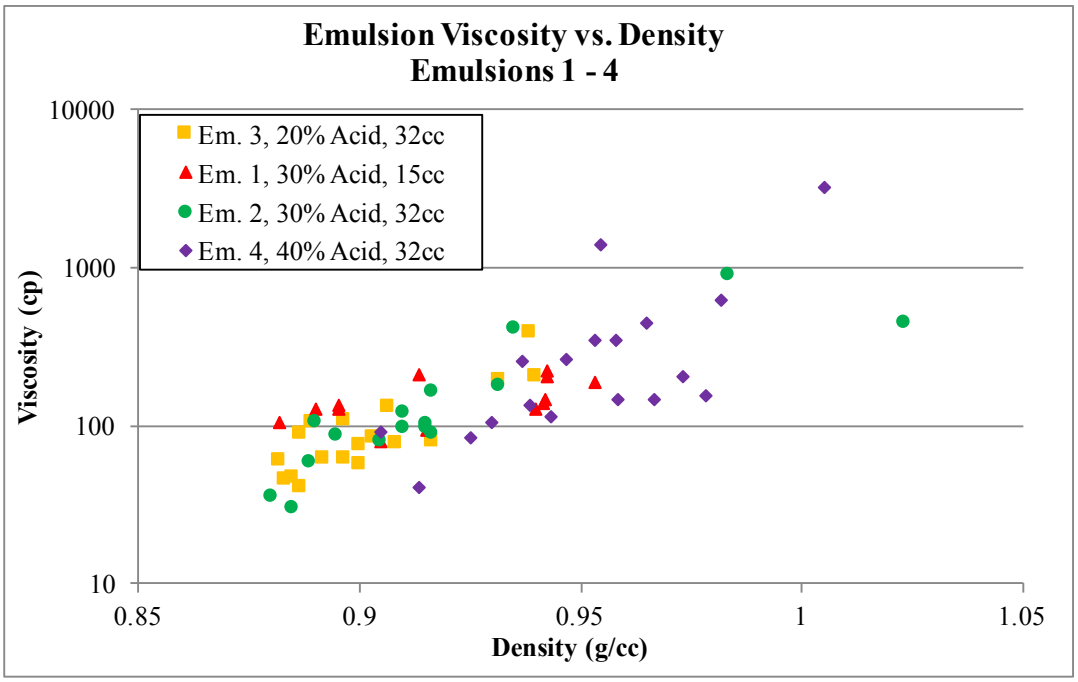

Figure 18: Emulsion Viscosity vs. Density, Emulsions 1-4

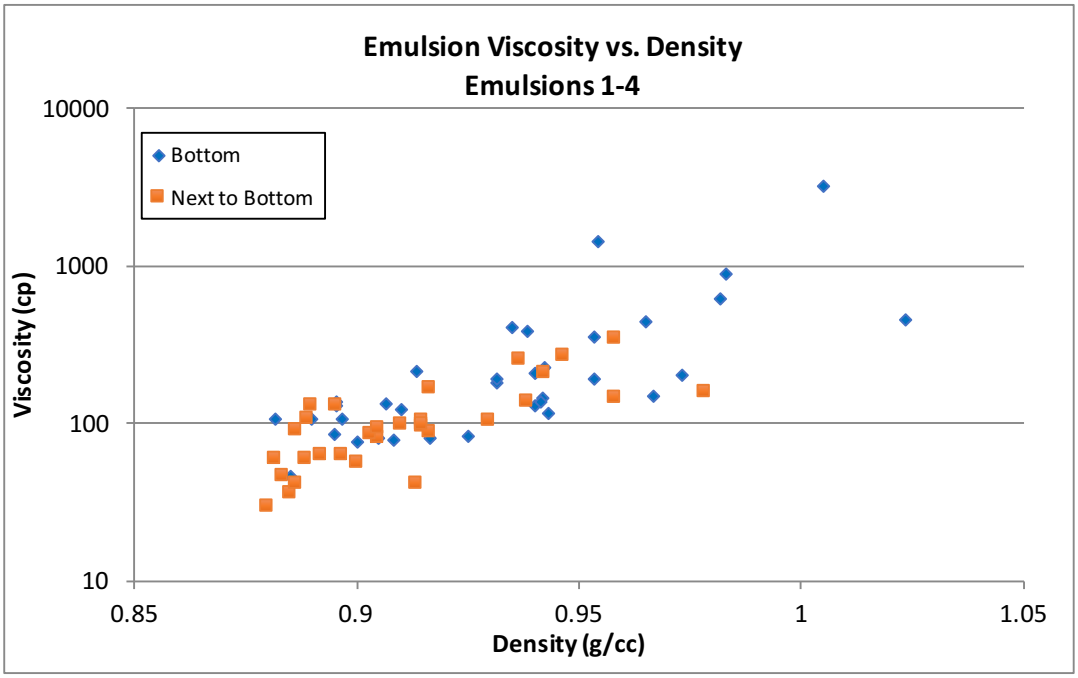

Figure 19: Emulsion Viscosity vs. Density, Measurement Type

In summary we see that acid-in-crude emulsion viscosity increases dramatically with acid fraction for the system studied. While the crude viscosity is only 25 cp, emulsion viscosities of several hundred centipoise or more are not uncommon. An extremely viscous, nearly solid portion separates out from each mixture within hours to days and is stable indefinitely. If a similar emulsion is formed in the rock matrix of a reservoir in any appreciable quantity it has the potential to damage the formation and decrease well productivity.

3.2 Coreflooding

Coreflooding experiments were conducted to study the formation of acid-in-oil emulsions during acid injection and any effect the emulsions may have on subsequent oil injection. Two main types of corefloods were conducted:

(1) Full wormhole propagation – acid injected through the core until acid breakthrough, differential pressure drops to zero. May be further divided into experiments with backpressure (1200 psi) and without backpressure.

(2) Partial wormhole propagation – acid injected through the core for a period of time (1 – 1.5 mins) shorter than the required breakthrough time. Oil is injected in the opposite direction and the pressure is recorded.

A matrix of experimental parameters is shown in **Table 6**. Acid is always injected at the rate of 3.5 cc/min and all experiments are at room temperature. The quantity PV_{bt}, or pore-volumes to breakthrough, is a dimensionless measure of the amount of acid needed to create a full wormhole through a core. It is defined as:

$$PV_{bt} = \frac{acid\ volume\ injected\ at\ breakthrough, cc}{core\ pore\ volume, cc}$$

Table 6: Coreflooding Experiment Matrix

Core	Fluid Sat.	Aging (days)	Wormhole Type	Back pressure (psi)	Oil Inj. Rate (cc/min)	Acid Inj. Time (min)	Acid Soak Time (hr)	PV_{bt}
LS-2	Crude	60	Full					0.35
LS-3			Full					1.32
LS-4	Crude	2	Full	1200				0.28
LS-5			Full	1200				0.51
LS-7	Crude	19	Full	1200				0.21
LS-8	DI water	15	Full	1200				0.30
LS-9	Crude	4	Partial	1200	0.5	1	-	
LS-10	Min. oil	31	Partial	1200	0.5	1	-	
LS-11	Crude	16	-	1200	0.3	-	-	
LS-12	Crude	14	Partial	1200	0.3	1	24	
LS-13	Crude	14	Partial	1200	0.3	1	-	
LS-14	Min. oil	14	Partial	1200	0.3	1	-	
LS-15	Crude	16	Partial	1200	0.3	1.5	24	

3.2a Full Wormhole Propagation (no Backpressure)

Cores LS-2 (crude) and LS-3 (unsaturated) were used in full wormhole propagation experiments without backpressure. An acid-in-crude emulsion, approximately 10 cc in volume, was produced from core LS-2 at breakthrough and collected at the outlet. The effluent fluid contained acid in the pH range 0-0.5 after production of the emulsion. Emulsion viscosity and density were measured as shown in **Table 7**. The emulsion is quite viscous, we can infer from the density and viscosity the acid volume fraction is high. The emulsion is also stable and shows a strong resistance to flow when the vial is turned. A sample of the emulsion is shown in **Figure 20** one week after collection. To the best of our knowledge there have been no reports in the literature of direct evidence for in-situ emulsification during acid coreflooding on crude saturated cores.

Table 7: Core LS-2 Effluent Emulsion Properties

Density (g/cc)	Viscosity (cp)
1.05	860

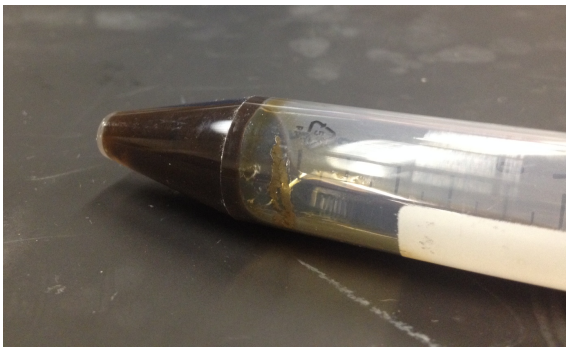

Figure 20: LS-2 Effluent Emulsion Sample at 1 Week

Core LS-2 (crude) has higher wormholing efficiency, or requires a lower volume of acid at breakthrough than core LS-3. The core differential pressures are shown in **Figure 21**; note the pressure exceeded that of the transducer for core LS-3 but the pump pressure was recorded. In a previous coreflooding study with oil-saturated cores, Al-Mutairi et al. theorized in-situ emulsion formation between HCl and crude slowed reaction rates and increased wormholing efficiency (Al-Mutairi, Al-Obied, Al-Yami et al. 2012). This is possible in our case as any emulsification of acid in crude is likely to

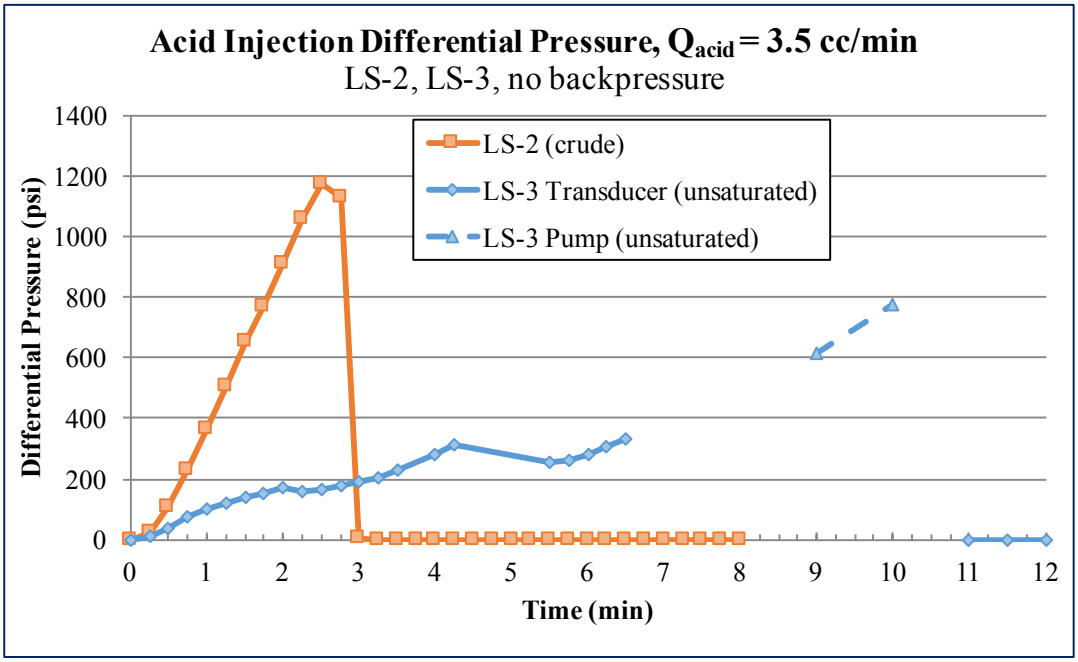

Figure 21: LS-2, LS-3 Acid Injection Differential Pressure

slow reaction rates. However, emulsion formation of this type could also have negative implications. For example, the formation of this type of emulsion in the matrix rock surrounding a wormhole could potentially block access to the wormhole and decrease well productivity.

3.2b Full Wormhole Propagation (1200 psi Backpressure)

Full wormhole propagation experiments were run with 1200 psi backpressure for cores LS-4 (crude), LS-5 (unsaturated), LS-7 (crude), and LS-8 (DI water). The inclusion of backpressure is meant to keep as much CO_2 generated from the reaction between the acid and rock in a liquid state. There was evidence of emulsion formation in corefloods LS-4 (crude) and LS-7 (crude), but it was more difficult to collect and measure than in the coreflood without backpressure; this is because the effluent fluid flowed to an accumulator under pressure. After breakthrough, the pressure in the system was released, first by increasing the volume of the accumulator to its maximum and then bleeding pressure from a needle valve. When pressure was released at the valve, a small volume of emulsion was produced. Some emulsion was also present in the outlet accumulator, but it tends to coat the accumulator surface and was difficult to collect enough volume for any type of measurement. Small acid-in-oil emulsion droplets are visible in the collected fluids for cores LS-4 and LS-7 in **Figure 22** and **Figure 23**, respectively. It is not clear if the volume of emulsion produced is less in the corefloods with backpressure, or if it was just more difficult to collect given the nature of the experimental setup.

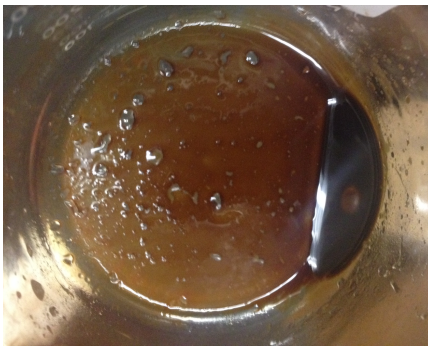

Fluid transferred from accumulator

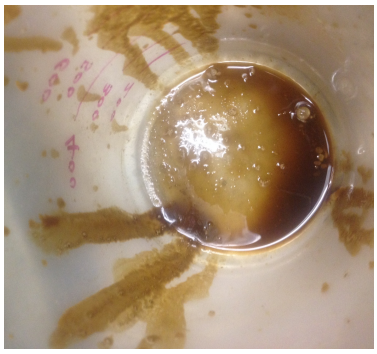

fluid collected during pressure bleed-off

Figure 22: Core LS-4 Effluent Emulsion

Fluid in accumulator

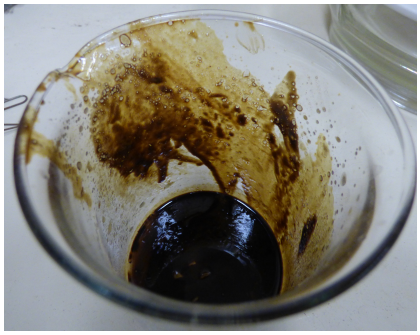

Fluid transferred from accumulator

fluid collected during pressure bleed-off

Figure 23: Core LS-7 Effluent Emulsion

A small leak at the core inlet was observed during the LS-7 coreflood. It seems the nitrogen gas applied at the outlet channeled through the core and exited a failing connection at the inlet. Some small oil droplets and gas bubbles were observed. This leak likely explains the difference in the slope of differential pressure between cores LS-4 and LS-7 as is shown in **Figure 24**. Also, data from 1.75 – 2.0 minutes is unavailable for core LS-4 due to a loose electrical connection on the pressure display. The pressure slope for the DI-water saturated core is less than the crude saturated cores, probably due to lower water vs. crude viscosity. Expectedly, the injection pressure for the unsaturated core, shown in **Figure 25**, is much less than the fluid saturated cores. In terms of wormholing efficiency, the crude saturated cores had the highest, followed by the water-saturated core, and then the unsaturated core.

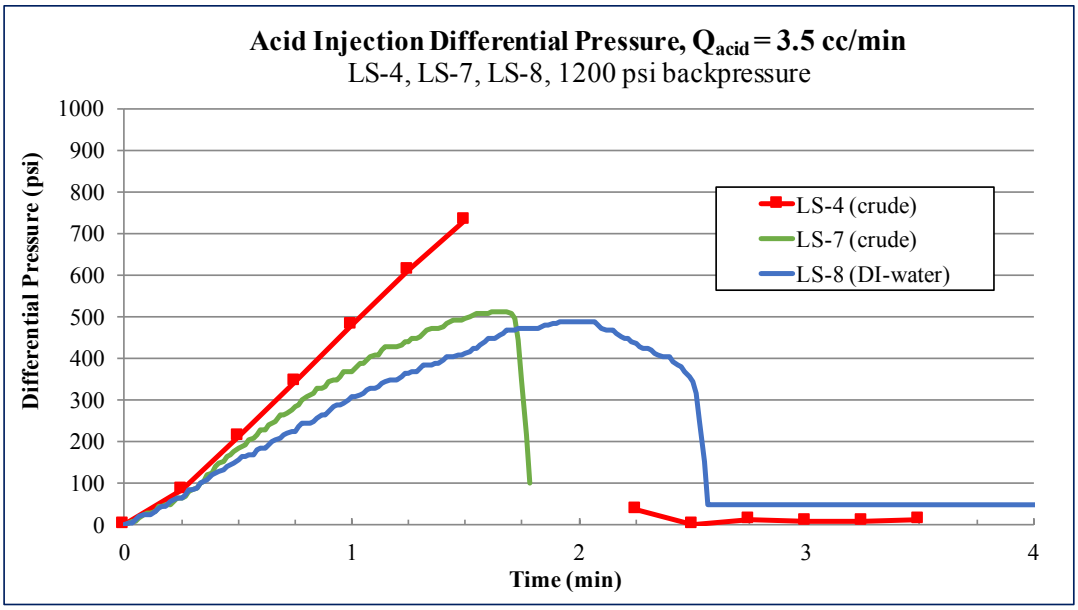

Figure 24: LS-4, LS-7, LS-8 Acid Injection Differential Pressure

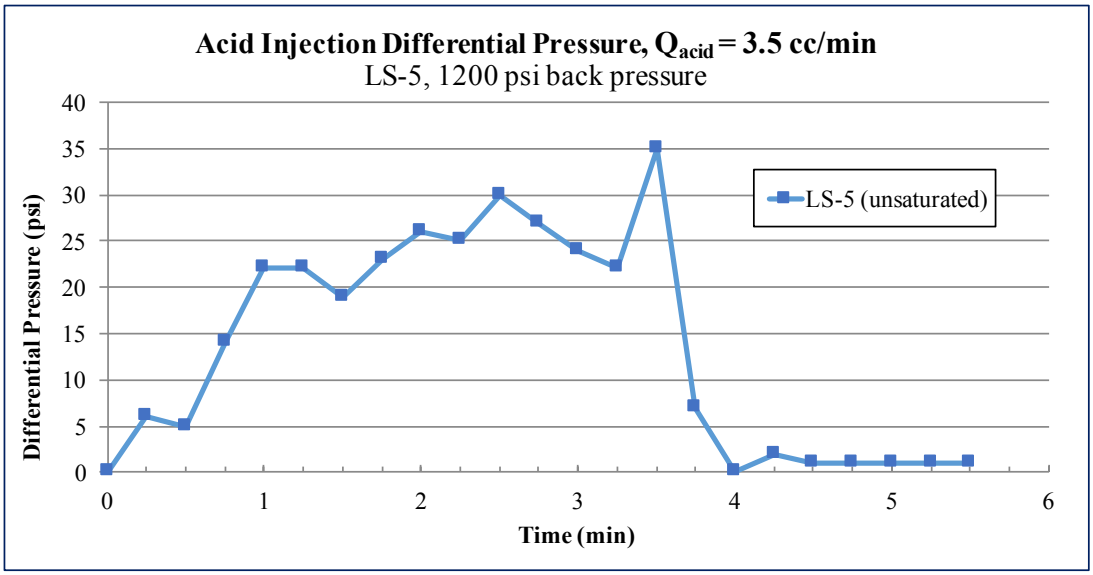

Figure 25: LS-5 Acid Injection Differential Pressure

3.2c Partial Wormhole Propagation and Oil Injection (Q_{oil} = 0.5 cc/min)

Acid was injected into cores LS-9 (crude) and LS-10 (mineral oil) for only 1 minute with subsequent oil (crude or mineral oil) injection in the opposite direction. Acid injection pressure for these cores is shown in **Figure 26.** The slope of acid injection pressure is higher in the case of mineral oil likely due to its slightly higher viscosity. The experiment objective was to test the effect of in-situ acid-in-crude emulsion formation on subsequent oil production. If emulsion formation in the crude-saturated core, LS-9, has a limiting effect on oil production, we should be able to observe a higher oil injection pressure with core LS-9 that with core LS-10. Note the viscosity of mineral oil, 32 cp, is slightly higher than that of the crude oil, 25 cp, and the cores likely have small differences in permeability.

Oil injection pressure following acid injection is not any higher with LS-9 (crude) than LS-10 (mineral oil) as is shown in **Figure 27**. Therefore, any detrimental effect of acid-crude emulsion formation is not observed. In fact, the injection pressure slope is higher with the mineral oil core; this may be partly due to higher mineral oil viscosity. Note that a pre-acid oil injection period was added to the procedure starting with core LS-10. Also, the maximum pump pressure was reached in both experiments so the oil injection rate was lowered from 0.5 to 0.3 cc/min for the subsequent corefloods.

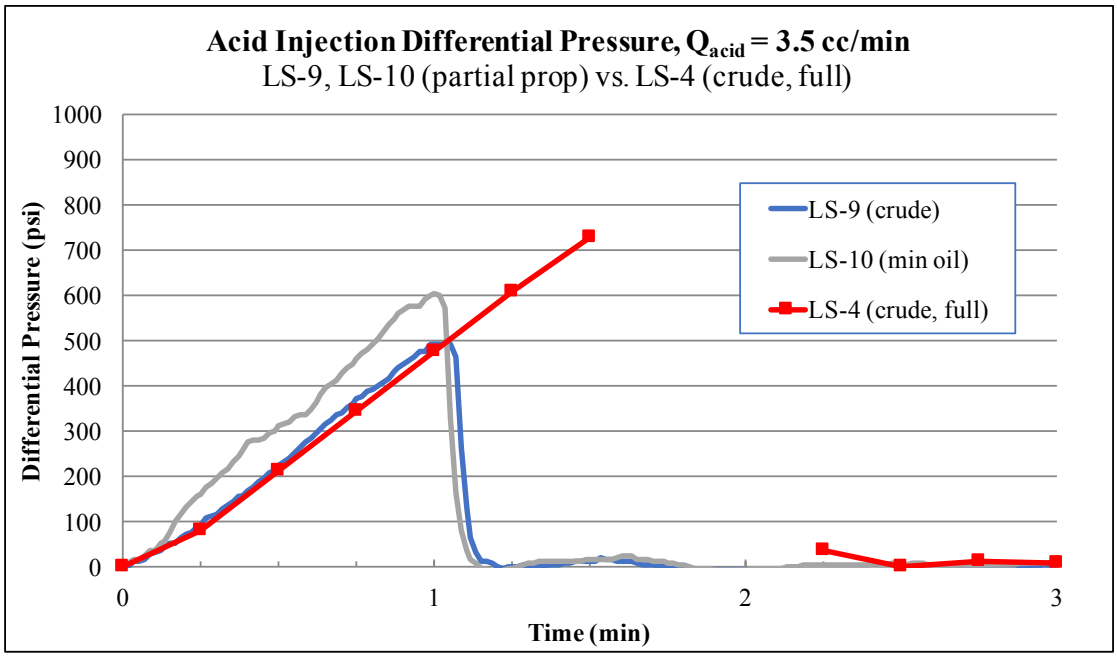

Figure 26: LS-9, LS-10 Acid Injection Differential Pressure

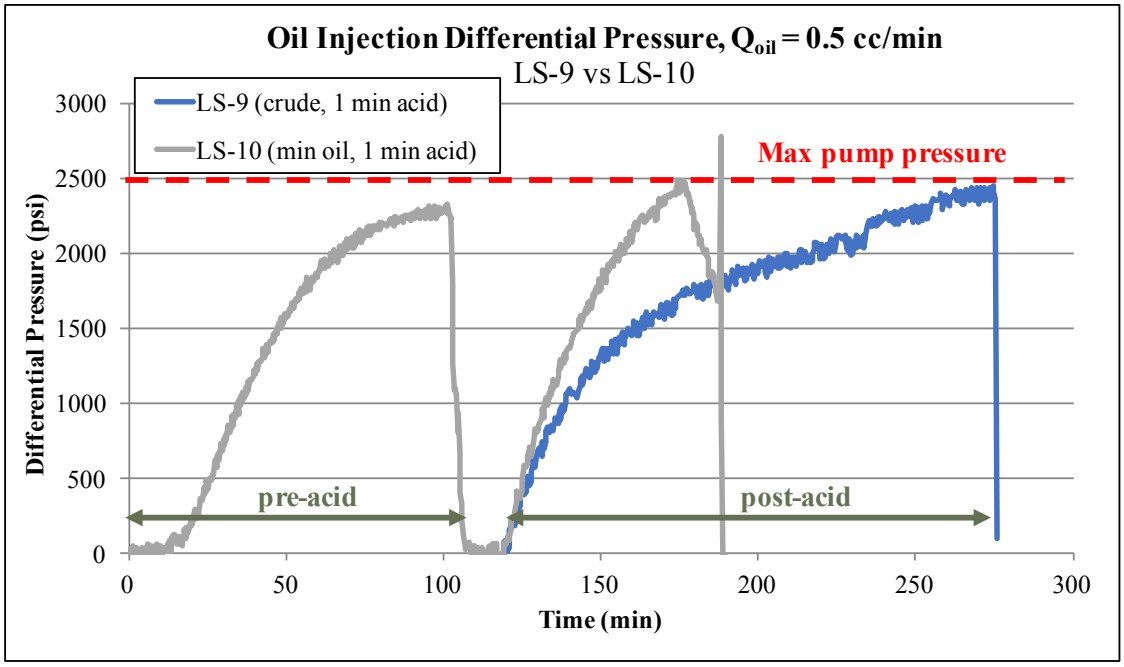

Figure 27: LS-9, LS-10 Oil Injection Differential Pressure

No dominant wormhole is not visible at the face of core LS-9 or core LS-10 as can be seen in **Figure 28** and **Figure 29**, respectively. It is theorized numerous very narrow wormholes are created and begin to propagate, but the exposure time to acid is short so the wormholes remain narrow. It is difficult to tell if this is this occurring, but one might make this interpretation from the pictures. An emulsion between the acid-crude and/or the oil-wet condition of the cores may delay acid-rock reaction resulting in many narrow wormholes.

Core LS-9 In Core LS-9 Out

Figure 28: Core LS-9 Inlet/Outlet

Figure 29: Core LS-10 Inlet/Outlet

3.2d Partial Wormhole Propagation and Oil Injection (Q_{oil} = 0.3 cc/min)

Acid was injected into cores LS-12 (crude, 24 hr acid soak), LS-13 (crude), and LS-14 (min oil) for 1 minute as shown in **Figure 30**. The acid injection period was increased to 1.5 minutes for core LS-15 (crude, 24 hr acid soak) since no clear wormhole patterns were observed on the previous cores; the acid injection period was stopped at 1.5 minutes, but due to a pump controller malfunction the controller had to be rebooted to reduce the inlet pressure back to 1200 psi. Because of this, the acid injected remains in the core under pressure for about 1.75 minutes.

Any impact of acid-crude emulsion formation on oil injection cannot be interpreted from the oil injection pressures seen in **Figure 31**. Again, if this were the case, we would expect a greater post-acid injection pressure in the crude saturated cores compared to the mineral oil saturated core. It is interesting the short acid injection period does not decrease the resistance to oil flow for any of the cores. A higher acid injection volume may be necessary to create wormholes with sufficient conductivity.

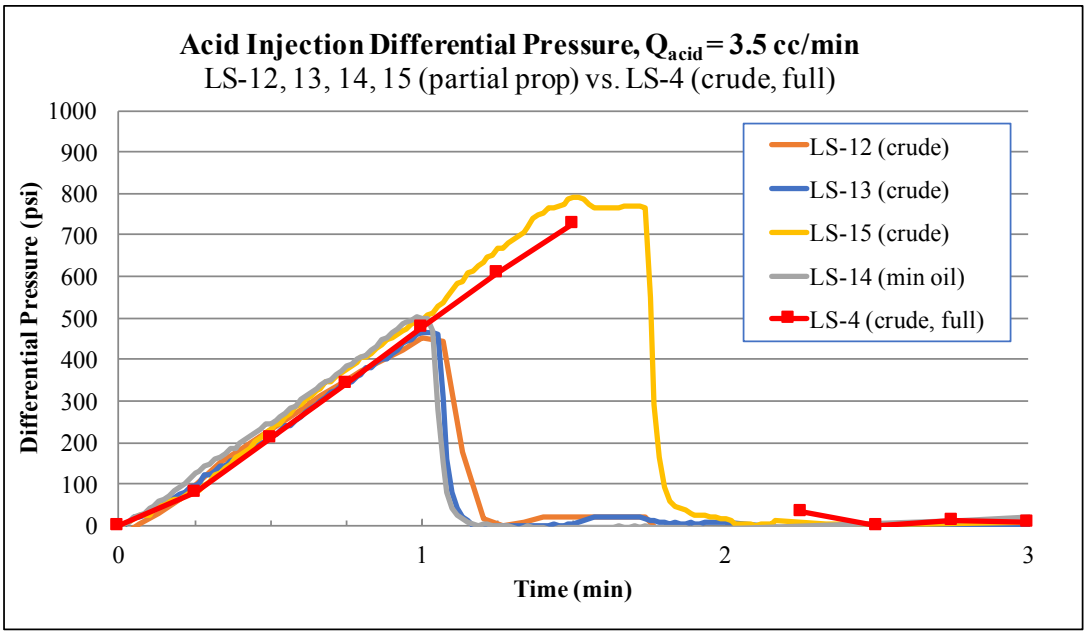

Figure 30: LS-12, 13, 14, 15 Acid Injection Differential Pressure

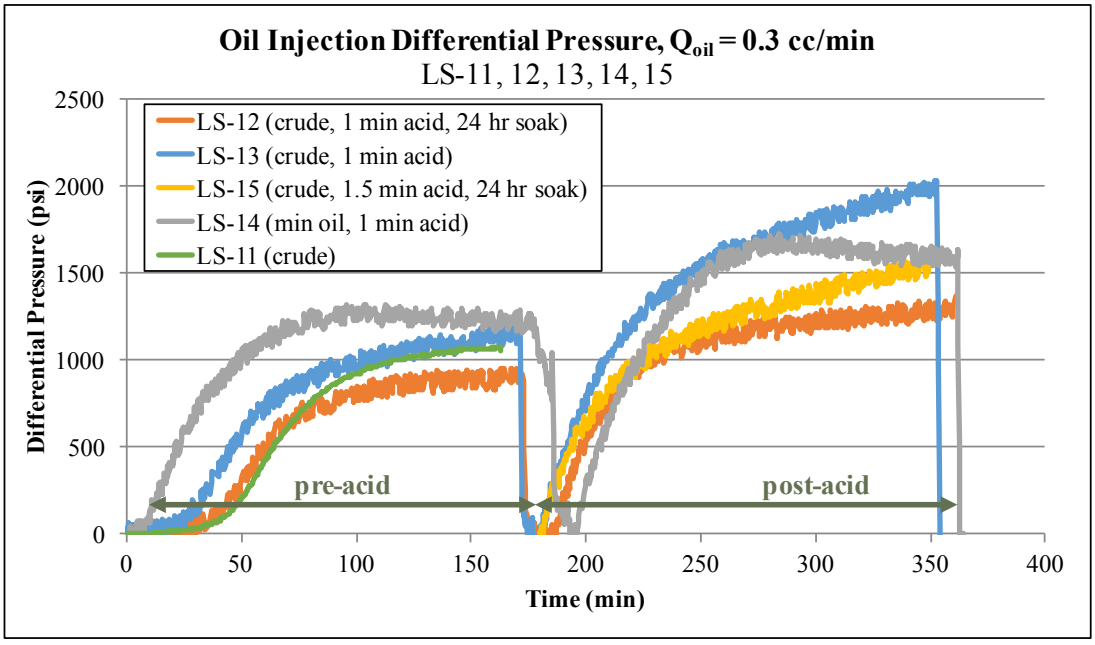

Figure 31: LS-11, 12, 13, 14, 15 Oil Injection Differential Pressure

Also, we can see core LS-14 (mineral oil) reaches a steady state pressure drop during both pre-acid and post-acid injection periods, but none of the crude saturated cores reach steady state during oil injection: there is a gradual increase in pressure during the second half of each injection period. The most likely explanation for this may be asphaltene deposition. It seems the core permeability is decreases with the total volume of injected crude.

No clear wormhole pattern is observed at the inlet face of any of the cores. In examing Core LS-15, shown in **Figure 32**, one might interpret the presence of many narrow wormholes at the core inlet, but a definitive observation cannot be made. In a coreflooding study with HCl and emulsified acids on carbonate cores, Buijse and van Domelen observe many narrow wormholes created in the rock when emulsified acids are used (Buijse and van Domelen 1998). We assume the creation of many narrow wormholes in the partial propagation test cores but more study is needed to substantiate this.

Figure 32: Core LS-15 Inlet/Outlet

In summary, the results of the partial propagation core tests are inconclusive. More study is needed on cores with full wormhole propagation to understand the wormhole geometry in oil saturated cores at the point of breakthrough. The two experiments performed on oil-saturated cores with full wormhole propagation (1200 psi backpressure) have limitations. For core LS-4, it had only aged 2 days before the test. For core LS-7 there was a leak which we believe aided the formation of one dominant wormhole. It is quite possible the wormhole geometry is very narrow at breakthrough. Also, a large proportion of the wormhole length could be created in a short time before breakthrough when the pressure gradient in the core is at a maximum. It would be interesting to repeat the full wormhole propagation experiment and at the exact point of breakthrough switch acid injection to deionized water injection to see exactly what the wormhole geometry at breakthrough looks like.

Alternatively, the partial propagation test could be repeated with acid injection until the differential pressure has reached a maximum and started to decrease. In this case we would more likely have a clear wormhole at the inlet. However, in most of our full propagation experiments, after the differential pressure reaches a maximum, it drops to zero extremely quickly, so it may be difficult to use this strategy without creating a full wormhole.

Also, performing the experiment at a lower acid injection rate it might make it easier to propagate a wormhole partially through the core as the acid would have more time to react with the rock. Changing the injection rate will likely affect the formation of emulsion but to what extent is not clear.

CHAPTER 4: CONCLUSIONS

The following conclusion are drawn based on the bottle testing study of the effect of acid volume fraction and time on emulsion viscosity and stability. Also, conclusions from the study of the in-situ emulsification in acid coreflooding on oil saturated cores and the effect on oil production is discussed:

- For the crude-acid system studied, a tight emulsion was produced. In hours to days after mixing, free oil tends to separate from the emulsion with time leaving a very viscous, quasi-solid emulsion with a higher acid volume fraction than initially mixed. After this initial separation the emulsion is stable indefinitely.
- Emulsion viscosity increases with increasing acid volume fraction. This was true for the emulsions measured immediately after mixing and for the emulsions which had been given time to separate.
- Emulsion viscosity increases with time for the system studied. Extremely high viscosities, several hundred cP to over 1000 cP, were measured hours to days after the emulsions had been mixed. This may suggest decreasing acid soaking times in some field application could be beneficial.
- The viscous emulsions observed in bottle testing have the potential to negatively impact well productivity if produced in the reservoir in any significant amount. This conclusion is supported by field reports in literature.
- A viscous, stable acid-in-crude emulsion was produced in-situ in a crude-saturated core in a coreflood without backpressure. To our knowledge this is the first direct evidence presented of in-situ emulsification in an acid coreflood.

- Qualitative observations suggest some amounts of in-situ acid-in-crude emulsions were produced in crude-saturated cores in corefloods with 1200 psi backpressure.
- Crude-saturated cores had a higher wormholing efficiency than the DI-water saturated core. Unsaturated cores had the lowest wormholing efficiency in the current study.
- Partial wormhole propagation and oil injection corefloods were inconclusive in quantifying an impact of in-situ emulsification on oil injection. Wormhole patterns in these tests are difficult to observe and it is theorized the acid enters many narrow channels in the core, but exposure time to acid is not high enough to create clearly visible wormholes.

Future Work

Future areas of investigation on the topic are listed below:

- Study the presence of solid precipitate in the acid-crude mixtures. For example, filter the emulsion through 100 mesh screen or study under microscope for evidence of asphaltene agglomerates.
- Improve the partial propagation and oil injection experiement. Perhaps the acid injection time needs to be increased.
    - More full wormhole propagation experiments with DI water injection at breakthough would increase understanding on the wormhole geometry
    - Acid could be injected until the pressure has reached a maximum and started to decrease. This will likely result in a clearer wormhole.

    - Partial propagation experiments at lower injection rate may be easier to execute although the effect of injection rate on emulsification may have an impact.
    - If suitable results are obtained showing a negative impact of emulsification on oil production, run similar experiments with preventative or remedial measures (demulsifier additive, organic solvents, etc.).
- Study the effect of injection rate on emulsion formation. It may be easiest to start with corefloods without backpressure.
- Study the effect of increased temperature on emulsion viscosity/stability in bottle testing and on emulsion formation in corefloods.
- Study effect of acid strength. Simple bottle tests suggest 28% HCl creates much tighter emulsions, maybe more precipitate

References

Abdel-Raouf, M.E. 2012. Factors Affection the Stability of Crude Oil Emulsions. Croatia: InTech. http://dx.doi.org/10.5772/35018.

Al-Mutairi, S.H., Al-Obied, M.A., Al-Yami, I. et al. 2012. Wormhole Propagation in Tar During Matrix Acidizing of Carbonate Formations. Presented at the SPE International Symposium and Exhibition on Formation Damage Control, 15-17 February, Lafayette, Louisiana, USA. SPE-151560-MS. http://dx.doi.org/10.2118/151560-MS.

Alvarado, D.A. and Marsden, S.S. 1979. Flow of Oil-in-Water Emulsions Through Tubes and Porous Media. *SPE J.* **19** (6): 369-377. SPE-5859-PA. http://dx.doi.org/10.2118/5859-PA.

Alvarado, V., Wang, X., and Moradi, M. 2011. Role of Acid Components and Asphaltenes in Wyoming Water-in-Crude Oil Emulsions. *Energy and Fuels* **25** (10): 4606-4616. http://dx.doi.org/10.1021/ef2010805.

Aske, N., Kallevik, H., and Sjöblom, J. 2002. Water-in-crude Oil Emulsion Stability Studied by Critical Electric Field Measurements. Correlation to Physico-chemical Parameters and Near-Infrared Spectroscopy. *Journal of Petroleum Science and Engineering* **36** (1): 1-17. http://dx.doi.org/10.1016/S0920-4105(02)00247-4.

Bazin, B. and Abdulahad, G. 1999. Experimental Investigation of Some Properties of Emulsified Acid Systems for Stimulation of Carbonate Formations. Presented at the Middle East Oil Show and Conference, 20-23 February, Bahrain. SPE-53237-MS. http://dx.doi.org/10.2118/53237-MS.

Buijse, M.A. and van Domelen, M.S. 1998. Novel Application of Emulsified Acids to Matrix Stimulation of Heterogeneous Formations. Presented at the SPE Formation Damage Control Conference, 18-19 February, Lafayette, Louisiana. SPE-39583-MS. http://dx.doi.org/10.2118/39583-MS.

Coppel, C.P. 1975. Factors Causing Upsets to Surface Facilities Following Acid Stimulation. *J Pet Technol* **27** (9): 1060-1066. SPE-5154-PA. http://dx.doi.org/10.2118/5154-PA.

deZabala, E.F. and Radke, C.J. 1986. A Nonequilibrium Description of Alkaline Waterflooding. *SPE Res Eng* **1** (1): 29-43. SPE-11213-PA. http://dx.doi.org/10.2118/11213-PA.

Dickie, J.P. and Yen, T.F. 1967. Macrostructures of the Asphaltic Fractions by Various Instrumental Methods. *Anal Chem*. **39** (14): 1847-1852. http://dx.doi.org/10.1021/ac50157a057.

Dunlap, D.D. and Houchin, L.R. 1990. Evaluation of Acid System Design and Formation Damage Using Polarized Microscopy. Presented at the SPE Formation Damage Control Symposium, 22-23 February, Lafayette, Louisiana. SPE-19425-MS. http://dx.doi.org/10.2118/19425-MS.

Eley, D.D., Hey, M.J., and Symonds, J.D. 1988. Emulsions of Water in Asphaltene-Containing Oils. 1. Droplet Size Distribution and Emulsification Rates. *Colloids and Surfaces* **32** (1988): 87-101. http://dx.doi.org/10.1016/0166-6622(88)80006-4.

Hashmi, S.M. and Firoozabadi, A. 2011. Tuning size and Electrostatics in Non-Polar Colloidal Asphaltene Suspensions by Polymeric Adsorption. *Soft Matter* **7** (18): 8384-8391. http://dx.doi.org/10.1039/c1sm05384a.

Houchin, L.R., Dunlap, D.D., Arnold, B.D. et al. 1990. The Occurrence and Control of Acid-Induced Asphaltene Sludge. Presented at the SPE Formation Damage Control Symposium, Lafayette, Louisiana, 22-23 February. http://dx.doi.org/10.2118/19410-MS.

Jacobs, I.C. 1989. Chemical Systems for the Control of Asphaltene Sludge During Oilwell Acidizing Treatments. Presented at the SPE International Symposium on Oilfield Chemisty, 8-10 February, Houston, Texas. SPE-18475-MS. http://dx.doi.org/10.2118/18475-MS.

Jacobs, I.C. and Thorne, M.A. 1986. Asphaltene Precipitation During Acid Stimulation Treatments. Presented at the SPE Formation Damage Control Symposium, Lafayette, Louisiana, 26-27 February. SPE-14823-MS. http://dx.doi.org/10.2118/14823-MS.

Jones, T.J., Neustadter, E.L., and Wittingham, K.P. 1978. Water-in-Crude Oil Emulsion Stability and Emulsion Destabilization by Chemical Demulsifiers. *J Can Pet Technol* **17** (2): 100-108. PETSOC-78-02-08. http://dx.doi.org/10.2118/78-02-08.

Kimbler, O.K., Reed, R.L., and Silberberg, I.H. 1966. Physical Characteristics of Natural Film Formed at Crude Oil-Water Interfaces. *J Pet Technol* **6** (2): 153-165. SPE-77497-PA. http://dx.doi.org/10.2118/1201-PA.

Knopp, M. 2009. Non-damaging Matrix and Fracturing Acids: Some Key Considerations, Richardson, Texas: Distinguished Lecturer Program, Society of Petroleum Engineers. http://www.spe.org/dl/docs/2009/Knopp.pdf

Kokal, S. 2005. Crude Oil Emulsions: A State-of-the-Art Review. Presented at the SPE Annual Technical Conference and Exhibition, 29 September-2 October, San Antonio, Texas. SPE-77497-MS. http://dx.doi.org/10.2118/77497-MS.

Krueger, R.F. 1988. An Overview of Formation and Well Productivity in Oilfield Operations: An Update. Presented at the SPE California Regional Meeting, 23-

25 March, Long Beach, California. SPE-17459-MS. http://dx.doi.org/10.2118/17459-MS.

Langevin, D., Poteau, S., Hénaut, I. et al. 2004. Crude Oil Emulsion Properties and their Application to Heavy Oil Transportation. *Oil & Gas Science and Technology* **59** (5): 511-521. http://ogst.ifpenergiesnouvelles.fr/articles/ogst/pdf/2004/05/langevin_vol59n5.pdf.

McLean, J.D. and Kilpatrick, P.K. 1997. Effects of Asphaltene Solvency on Stability of Water-in-Crude Oil Emulsions. *Journal of Colloid and Interface Science* **189** (2): 242-253. http://dx.doi.org/10.1006/jcis.1997.4807.

Mirvakili, A., Rahimpour, M.R., and Jahanmiri, A. 2012. Effect of a Cationic Surfactant as a Chemical Destabilization of Crude Oil Based Emulsions and Asphaltene Stabilized. *Journal of Chemical and Engineering Data* **57** (6): 1689-1699. http://dx.doi.org/10.1021/je2013268.

Moore, E.W., Crowe, C.W., and Hendrickson, A.R. 1965. Formation, Effect and Prevention of Asphaltene Sludges During Stimulation Treatments. *J Pet Technol* **17** (09): 1023-1028. SPE-1163-PA. http://dx.doi.org/10.2118/1163-PA

Mullins, O.C. 2011. The Asphaltenes. *Annu. Rev. Anal. Chem.* **4** (1): 393-418. 21689047. http://dx.doi.org/doi:10.1146/annurev-anchem-061010-113849.

Oluwatosin, I. 2016. Experimental Study of the Rheology and Stability Behavior of Surfactant Stabilized Water-in-oil Emulsion. MS Thesis, University of Oklahoma, Norman, Oklahoma (December 2016).

Omole, O. and Falode, O.A. 2005. Effects of Mixing Conditions, Oil Type and Aqueous Phase Composition on Some Crude Oil Emulsions. *Journal of Applied Sciences* **5** (5): 873-877. http://198.170.104.138/jas/2005/873-877.pdf.

O'Niel, B., Maley, D., and Lalchan, C. 2015. Prevention of Acid-Induced Asphaltene Precipitation: A Comparison of Anionic vs. Cationic Surfactants. *J Can Pet Technol* **54** (1): 49-62. SPE-164087-PA. http://dx.doi.org/10.2118/164087-PA.

Picou, R.A., Ricketts, K., Luquette, M. et al. 1992. Successful Stimulation of Acid-Sensitive Crude Producers in the Gulf of Mexico. Presented at the SPE Formation Damage Control Symposium, 26-27 February, Lafayette. SPE-23818-MS. http://dx.doi.org/10.2118/23818-MS.

Rae, P. and Di Lullo, G. 2003. Matrix Acid Stimulation: A State-of-the-Art Review. Presented at the SPE European Formation Damage Conference, 13-14 May, The Hague, Netherlands. SPE-82260-MS. http://dx.doi.org/10.2118/82260-MS.

Rietjens, M. 1997. Sense and Non-Sense about Acid-Induced Sludge. Presented at the SPE European Formation Damage Conference, The Hague, Netherlands, 2-3 June. SPE-38163-MS. http://dx.doi.org/10.2118/38163-MS.

Sayed, M.A., Assem, A.I., and Nasr-El-Din, H.A. 2014. Effect of Oil Saturation on the Flow of Emulsified Acids in Carbonate Rocks. *SPE Prod & Oper* **29** (1): 29-41. SPE-152844-PA. http://dx.doi.org/10.2118/152844-PA.

Soo, H. and Radke, C.J. 1984. The Flow Mechanism of Dilute Stable Emulsions in Porous Media. *Ind. Eng. Chem. Fundamen.* **23** (2): 342-347. http://dx.doi.org/10.1021/i100015a014.

Soo, H. and Radke, C.J. 1984. Velocity Effects in Emulsion Flow Through Porous Media. *Journal of Colloid and Interface Science* **102** (2): 462-476. http://dx.doi.org/10.1016/0021-9797(84)90249-2.

Soo, H and Radke, C.J. 1986. A Filtration Model for the Flow of Dilute Stable Emulsions in Porous Media – I. Theory. *Chemical Engineering Science* **41** (2): 263-272. http://dx.doi.org/10.1016/0009-2509(86)87007-5.

Strassner, J.E. 1968. Effect of pH on Interfacial Films and Stability of Crude Oil-Water Emulsions. *J Pet Technol* **20** (3): 303-312. SPE-1939-PA. http://dx.doi.org/10.2118/1939-PA.

Sztukowski, D.M., Jafari, M., Alboudwarej, H. et al. 2002. Asphaltene Self-Association and Water-in-Hydrocarbon Emulsions. *Journal of Colloid and Interface Science* **265** (1): 179-186. http://dx.doi.org/10.1016/S0021-9797(03)00189-9.

Yang, X., Verruto, V.J., and Kilpatrick, P.K. 2007. Dynamic Asphaltene Resin Exchange at the Oil-Water Interface: Time-Dependent W/O Emulsion Stability for Asphaltene/Resin Model Oils. *Energy and Fuels* **21** (3): 1343-1349. http://dx.doi.org/10.1021/ef060465w.

Yarranton, H.W., Hussein, H., and Masliyah, J.H. 2000. Water-in-Hydrocarbon Emulsions Stabilized by Asphaltenes at Low Concentrations. *Journal of Colloid and Interface Science* **228** (1): 52-63. http://dx.doi.org/10.1006/jcis.2000.6938.